Available online at www.sciencedirect.com
SCIENCE DIRECT®
Thermochimica Acta 411 (2004) 149–169
thermochimica acta
www.elsevier.com/locate/tca

Mechanistic modeling of the reaction kinetics of phenyl glycidyl ether (PGE) + aniline using heat flow and heat capacity profiles from modulated temperature DSC

Steven Swier, Bruno Van Mele*

Department of Physical Chemistry and Polymer Science—FYSC (TW), Vrije Universiteit Brussel—VUB, Pleinlaan 2, B-1050 Brussels, Belgium

Received 25 March 2003; received in revised form 25 July 2003; accepted 12 August 2003

Abstract

Modulated temperature DSC (MTDSC) has been performed on phenyl glycidyl ether (PGE) + aniline in order to obtain the non-reversing heat flow and heat capacity profiles simultaneously in a wide range of cure temperatures and mixture compositions. The epoxy (PGE) conversion as determined from the former signal corresponds to the one obtained from separate high performance liquid chromatography (HPLC), while the latter signal contains information on the individual reaction steps. Optimized kinetic parameters using a mechanistic approach, including both reactive and non-reactive complexes can successfully simulate MTDSC measurements for isothermal reaction temperatures ranging from 50 to 120 °C and for non-isothermal experiments with mixture compositions corresponding to concentrations of aniline in a range from 1.68 to 6.53 mol kg^{-1}. Concentration profiles for three mixture compositions as obtained from HPLC are also well predicted. The activation energies for the primary amine and secondary amine–epoxy reaction catalyzed by hydroxyl groups are 50 and 52 kJ mol^{-1}, respectively, while the initiation of the reaction corresponds to the primary amine–epoxy reaction catalyzed by primary amine groups with an activation energy of 72 kJ mol^{-1}. A negative substitution effect can be calculated at 0.18 from the ratio of secondary amine to primary amine–epoxy reaction rate constants.

Keywords: Modulated temperature differential scanning calorimetry; Heat capacity; Reaction kinetics; Epoxy–amine; Mechanistic model

1. Introduction

In order to improve the cure schedule during processing of epoxy resins, an accurate reaction kinetics model is essential. Much of the confusion in literature about the values of the reaction rate constants arises from the fact that different reaction mechanisms are used resulting in different rate equations. Empirical approaches in which the global conversion of epoxide groups is connected to the overall conversion rate can be used to simulate the effect of cure temperature on the reaction rate, but they are inadequate in predicting changes in reaction rate due to mixture composition and chemistry [1–4]. Semi-empirical models include parameters to distinguish between the primary amine and secondary amine–epoxy reaction steps, but often assume them to have equal reaction rate constants to simplify the equations [5,6]. The difference between the rate of the epoxy ring's opening under the effect of primary and secondary amine groups, termed substitution effect (or reactivity ratio), does exist in most systems and has to be included to understand the morphology development during network formation [7]. Therefore, a mechanistic approach resulting in values for all important kinetic reaction steps is preferable. There is disagreement in the literature concerning the reactivity ratios: values from 0.1 to 1.0 have been reported [8]. Moreover, the ratio is generally reported to be temperature independent, whereas some authors find an increasing trend with cure temperature [9,10]. To be able to compare literature results, however, the substitution effect should be defined as the ratio of the consumption rates of epoxide groups by secondary and primary amine functionalities [11]. Moreover, model kinetic studies of epoxy–amine systems are frequently performed in solvents like alcohol, which can selectively affect the reaction rate of both amine–epoxy reactions, and are also mostly studied solely for stoichiometric mixtures [12,13]. Marsella and Starner studied both

* Corresponding author. Tel.: +32-2-629-3276/3288; fax: +32-2-629-3278.
E-mail address: bvmele@vub.ac.be (B. Van Mele).

0040-6031/$ – see front matter © 2003 Elsevier B.V. All rights reserved.
doi:10.1016/j.tca.2003.08.009

aromatic and aliphatic amines in combination with epoxies and concluded that the former exhibited a negative substitution effect while the latter showed a marked positive substitution effect [14]. An additional complication in cure studies of commercial (network) systems relates to diffusion effects arising because curing has to be performed below the final glass transition [3,4]. Moreover, commercial systems contain reactive and non-reactive additives for which the concentration and chemical structure are difficult to obtain, interfering with a transparent mechanistic approach.

This can be avoided by using model, low-T_g epoxy–amine systems for which the reaction is chemically-controlled and the chemical structure resembles that of commercial systems. Since epoxy resins combined with aromatic amines are widely used as a thermoset material, phenyl glycidyl ether (PGE) + aniline has proven to be a good candidate in this respect [9,11,12,15,16]. One of the early works on this system investigated the different steps in the reaction mechanism by synthesizing the intermediate components in the reactive mixture [17]. In principle, only primary amine–epoxy and secondary amine–epoxy reaction steps should be considered for the reaction kinetics of this model system since reactions like homopolymerization and etherification only take place when specific catalysts are present or when cure is performed at elevated temperatures [6,18]. For PGE + aniline in particular, this has been checked by spectroscopy and chromatography [11,19]. Thus, the following basic steps apply for this system:

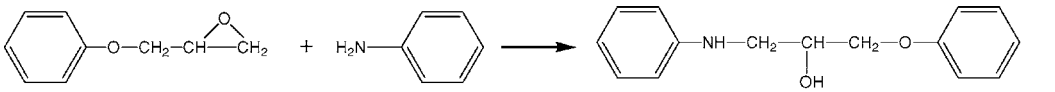

phenyl glycidyl ether (**E**) aniline ($\mathbf{A_1}$) N-(3-phenoxy-2-hydroxypropyl)aniline ($\mathbf{A_2}$)

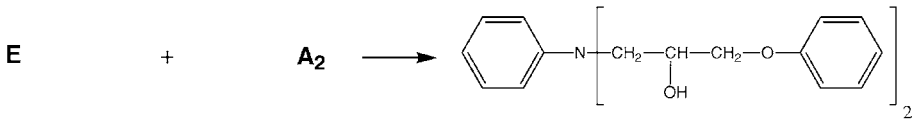

N,N-bis(3-phenoxy-2-hydroxypropyl)aniline ($\mathbf{A_3}$)

The formation of numerous intermediate complexes arising from donor–acceptor interactions, however, renders the reaction mechanism more complex [20]. In fact, the reaction of an amine group with an epoxide group occurs through the formation of a termolecular intermediate with a hydroxyl group formed during the reaction (autocatalysis) [21,22]:

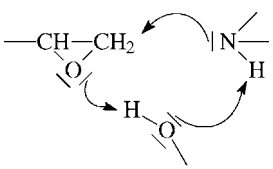

(EOH + $A_{1\,or\,2}$)

The initial reaction rate, however, has been found to be proportional to the square of the amine concentration [23,24]. This means that the uncatalyzed reaction, for which a dependency in first order with the amine concentration is expected, has a negligible contribution. An analogous termolecular intermediate has been proposed by replacing hydroxyl groups by primary amines, pointing out that the amine acts both as an electrophilic and as a nucleophilic reagent when hydroxyl groups are absent. Note that this reaction is termed “uncatalyzed” in some work, although the amine does act as a catalyst. For epoxy–amine systems containing impurities like water, the initial reaction rate is found to be closer to first order in primary amine concentration, reflecting the stronger catalytic effect of hydroxyl containing compounds. Beyond these initial stages of the reaction, the above mentioned autocatalytic reaction step therefore predominates the reaction kinetics [20]. To describe the final stages of the reaction, Mijovic et al. have proposed a second type of catalyzed reaction step in which both the epoxy and the amine itself form a transition complex with the formed hydroxyl groups, leading to a pseudo-tetramolecular reaction [15]. The probability of this reaction step is, however, questionable, since in forming the amine–hydroxyl complex, the lone pair electrons of the amine nitrogen would already be involved in bond formation, thereby losing its ability to attack the α-carbon atom of the epoxide oxirane group [25].

Apart from the hydrogen bond complexes which can participate in the reaction—epoxy–amine, epoxy–hydroxyl and amine–hydroxyl—other complexes could also exert influence [20,26]. It has been stated that self-associates such as epoxy–epoxy and amine–amine may be neglected in a kinetic analysis since such complexes do not result in significant changes in the reaction rate [27,28]. Complexes specific to certain epoxy–amine chemistries should not, however, be overlooked. In case of PGE, the ether groups form hydrogen bonds with the amine and hydroxyl groups of the reactive mixture which could therefore be deactivated to some extent [29,30]. Possible cyclic associates from intramolecular interaction between the secondary and tertiary amine groups with hydroxyl groups or ether groups are negligible (1–2%) [20].

Comparing studies using different experimental techniques should be done with care [31]. Infrared spectroscopy, for example, directly measures the concentration of reactive species after making the assumption of constant

absorptivity of the reactive medium during the reaction and after deciding upon a baseline for peak integration in combination with appropriate reference bands. This also means that the later stages of cure are difficult to monitor. On the other hand, while the epoxy and amine (N–H) functionalities can be readily distinguished, the absorption peaks for primary, secondary and tertiary amine groups have to be deconvoluted, which holds extra assumptions [32–34]. Near-IR spectroscopy, resulting in simplified spectrums, is better suited to quantify the concentration profiles of epoxy–amine systems [35]. Some of these issues can also be resolved by using Raman spectroscopy [36,37]. In the case of model epoxy–amine systems in which the reactive mixture stays soluble in the appropriate solvents throughout the reaction, chromatographic methods are very useful in separating all reactive species and determining their concentrations in combination with, for example, UV spectrometry [13,15,19]. The use of this technique for commercial network systems is restricted to the early stages of reaction since an insoluble fraction is formed at the gel point. Only the sol fraction can be analyzed beyond this point.

Cure schedules with accurate temperature control, which can be difficult to achieve for both spectroscopic and chromatographic techniques, are crucial for a kinetic study. While the former can be done in situ by using specially designed temperature chambers or by introducing fibres in the actual cure set-up [38], the latter is an inherently ex situ technique. Apart from the instabilities in the average temperature, any temperature distribution inside the sample should also be avoided. Calorimetric techniques like DSC, with optimal temperature control and small sample sizes, obviously do not pose these problems [39]. However, this technique can only obtain the global conversion of the reaction, mostly stated to correspond to the epoxy conversion, and will therefore not pose enough restrictions upon kinetic parameters in a mechanistic approach [40]. Modulated temperature DSC (MTDSC), however, offers additional information as concluded from a thermodynamic study of the epoxy–amine reaction [41]. It was shown that the global conversion from the heat flow signal indeed corresponds to the epoxy conversion, while the heat capacity signal is potentially interesting for distinguishing between the primary amine–epoxy and secondary amine–epoxy reaction steps. This will be further explored in this paper by evaluating the signals from MTDSC as an input for a mechanistic model of the reaction kinetics for PGE + aniline. The monofunctional reactant PGE is selected for its chemical resemblance to the constituents of thermosetting reactions: PGE represents half of a diglycidyl ether of bisphenol A (DGEBA) unit with the advantage of remaining soluble and amenable to analysis. High performance liquid chromatography will be used to assess the validity of the simulated concentration profiles.

2. Experimental

2.1. Materials

Phenyl glycidyl ether (PGE, $M_w = 150.2\,g\,mol^{-1}$, purity = 99%) and aniline ($M_w = 93.2\,g\,mol^{-1}$, purity = 99%) were obtained from Aldrich. The secondary amine *N*-(3-phenoxy-2-hydroxypropyl)aniline (A_2, $M_w = 243.3\,g\,mol^{-1}$) was obtained through the reaction of the system PGE + aniline of 1/10 molar ratio for 2 h at 80 °C. Aniline was redistilled under reduced pressure. The product was recrystallized from hexane/ether (needles, m.p. 60 °C). The ^{13}C NMR spectrum confirms the structure [12]. The tertiary amine *N*,*N*-bis(3-phenoxy-2-hydroxypropyl)aniline (A_3, $M_w = 393.5\,g\,mol^{-1}$) was obtained from the reaction of a stoichiometric mixture of PGE + aniline till reaction completion at 120 °C. Using preparative HPLC, Fryauf et al. were able to separate both diastereoisomeric forms. One form exists in needles (m.p. 83–84 °C) and the other form exhibits plates (m.p. 92–93 °C) [19]. No attempt was made here to separate the diastereoisomers, occurring in a 1/1 ratio [13]. HPLC was used, however, to confirm that only the tertiary amine remained after reaction at 120 °C. The ^{13}C NMR spectrum of A_3 is in agreement with literature. It shows splitting of similar intensities for the carbon atoms near the central nitrogen atom due to the presence of the diastereoisomeric pair [12]. Infrared spectra on both A_2 and A_3 further confirm their structure. Reactions of PGE with the model secondary amine A_2 allow the investigation of the secondary amine–epoxy reaction. Appropriate amounts of both components were introduced directly in a hermetic crucible. A pre-melt step at 65 °C for 5 min was included to assure a homogeneous mixture prior to the MTDSC experiments.

2.2. Modulated temperature DSC (MTDSC)

The TA Instruments 2920 DSC with MDSC™ option and a Refrigerated Cooling System (RCS) was used for MTDSC measurements. Samples ranging from 5 to 10 mg were measured using hermetic crucibles (the choice of pan-type has been discussed previously [41]). Helium was used as a purge gas ($25\,ml\,min^{-1}$). Indium and cyclohexane were used for temperature and enthalpy calibration. Heat capacity calibration was performed with a PMMA standard (supplied by Acros) using the heat capacity difference between two temperatures (one above and one below the glass transition temperature of PMMA [42]) to make sure that heat capacity changes were adequately measured. Quasi-isothermal measurements of the reaction enthalpy and heat capacity used a modulation amplitude of 1 °C in combination with a period of 60 s. Isothermal MTDSC measurements were obtained by quickly (at $30\,°C\,min^{-1}$) heating the reactive mixture to the cure temperatures of interest. This restricts the equilibration time needed to obtain the first reliable data point at T_{cure}.

2.3. High performance liquid chromatography (HPLC)

Separations were performed by reversed-phase (RP) HPLC using a Waters chromatographic system, which consisted of a low-pressure gradient with a Waters™ 600 Controller, a photodiode-array detector type 996 and an autosampler type Waters™ 717. Samples (20 μl) were injected at room temperature on an analytical RP column, Vydac 218TP54 C18, 250 mm × 4.6 mm i.d. (5 μm particle size) equipped with a guard column filled with identical material (The Separations Group). HPLC analyses were done by gradient elution with a flow rate of 1.0 ml min^{-1}. The mobile phase consisted of two components. Component A was a 70:30 (v/v) mixture of 0.01% (v/v) aqueous trifluor acetic acid (TFA) and 0.01% (v/v) TFA in acetonitrile. Component B was 0.01% (v/v) TFA in acetonitrile. The gradient ranged from 0% (v/v) A to 100% (v/v) B within 30 min. The HPLC system was also coupled to a VG Quattro II triple quadrupole mass spectrometer with an electrospray ionization (ESI) interface (Micromass).

To ensure that samples from MTDSC and HPLC were subjected to the same cure history, reacted PGE + aniline mixtures were taken directly from crucibles cured in MTDSC as samples for HPLC analysis.

A Perkin-Elmer Lambda 40 UV-Vis spectrometer, operating in a wavelength range from 190 to 1100 nm, was used to obtain reference spectra for the HPLC analysis. The radiation sources consisted of prealigned deuterium and halogen lamps, while a photodiode served as detector.

2.4. Optimization software for reaction kinetics modeling (FITME)

A mechanistic kinetic model is a stiff set of coupled differential equations describing the evolution of concentrations of the different species as a function of time. The software package FITME enables simulations and kinetic parameter optimizations. FITME is based on OPTKIN, a program for mechanistic modeling using kinetic and thermodynamic parameter optimization [43]. Multiple experiments can be optimized simultaneously with one parameter set.

The experimental input and output data of the program can be the heat flow and heat capacity during reaction, obtained via MTDSC, or concentration profiles, obtained via HPLC. Also note that the experimental temperature profile of the sample can be loaded to the program. The integration routine uses a 4th order semi-implicit Runge–Kutta method [44,45]. The optimization routine used [46] is based on a combination of three algorithms for finding the least square root: Newton–Raphson, Steepest Descent and Marquardt.

3. Results and discussion

3.1. Reaction mechanism

Using the reaction steps as elaborated in Section 1, the following mechanism can be proposed for the model system PGE + aniline [15,20] (Scheme 1): with E the epoxy, A_1 and A_2 the primary and secondary amine, respectively, and OH the hydroxyl group formed during the reaction; Cat designates catalysts OH and A_1; ECat is an equilibrium complex that can further react with A_1 or A_2 (termed *reactive* complex); the notation for the equilibrium constant (K) and reaction rate constants (k) with their respective activation energies (E) and pre-exponential factors (A) are also given. Model studies of both PGE + aniline and PGE + *N*-methylaniline have shown that the reactions of A_1 and A_2 with ECat are rate determining [11,25]. Other *non-reactive* complexes have to be considered between OH and A_1 and the ether group of the epoxy (Et) [20,26]. While the reactive complexes (EOH and EA_1) facilitate the reaction causing an accelerated rate, these non-reactive complexes will reduce the concentration of other reactive species and thus retard the reaction.

reactive complexes:

E + Cat	¾	ECat	K_{ECat}

primary and secondary amine-epoxy reaction:

ECat + A_1	⟶	OH + A_2 + Cat	k_{1Cat} (A_{1Cat}, E_{1Cat})
ECat + A_2	⟶	OH + A_3 + Cat	k_{2Cat} (A_{2Cat}, E_{2Cat})

non-reactive complexes:

A_1 + OH	¾	A_1OH	K_{A1OH}
Et + OH	¾	EtOH	K_{EtOH}
Et + A_1	¾	EtA_1	K_{EtA1}

Scheme 1.

$$E + A_1 + Cat \longrightarrow OH + A_2 + Cat \qquad k'_{1Cat}(A'_{1Cat}, E'_{1Cat})$$

$$E + A_2 + Cat \longrightarrow OH + A_3 + Cat \qquad k'_{2Cat}(A'_{2Cat}, E'_{2Cat})$$

Scheme 2.

Note that the amine–epoxy reaction can be depicted as a pseudo-trimolecular step, consisting of two successive bimolecular reactions over a transition complex (Scheme 2).

This notation is mostly used in literature to simplify the kinetic equations. In the case the reaction of ECat with A_1 and A_2 is slow in comparison to the equilibrium formation, the equilibrium constant K_{ECat} relates both rate constants: $k'_{i\,Cat} = K_{ECat} k_{i\,Cat}$ (for $i = 1$ and 2). Other possible reaction steps (uncatalyzed reactions, etherification, homopolymerization) and complexes were neglected as will be confirmed by experimental and optimization results in the following sections.

3.2. Experimental input

3.2.1. Concentrations of reactive groups as determined by HPLC

As an example, the chromatograms of a PGE + aniline mixture containing an excess in epoxide groups, cured for different times at 100 °C, are depicted in Fig. 1. Starting from a mixture of PGE (E) and aniline (A_1), the secondary amine (A_2) is formed first followed by the formation of the tertiary amine (A_3). Both diastereoisomers are clearly separated and turn out to form with equal probability (reaction does not show stereospecificity). For the calculation of concentration profiles of A_3, these peaks will be added together. The identification of the peaks in Fig. 1 has been performed by comparing the UV-Vis spectra at the retention times of interest with those on the individual pure components. On the basis of these spectra, wavelengths were selected in order to

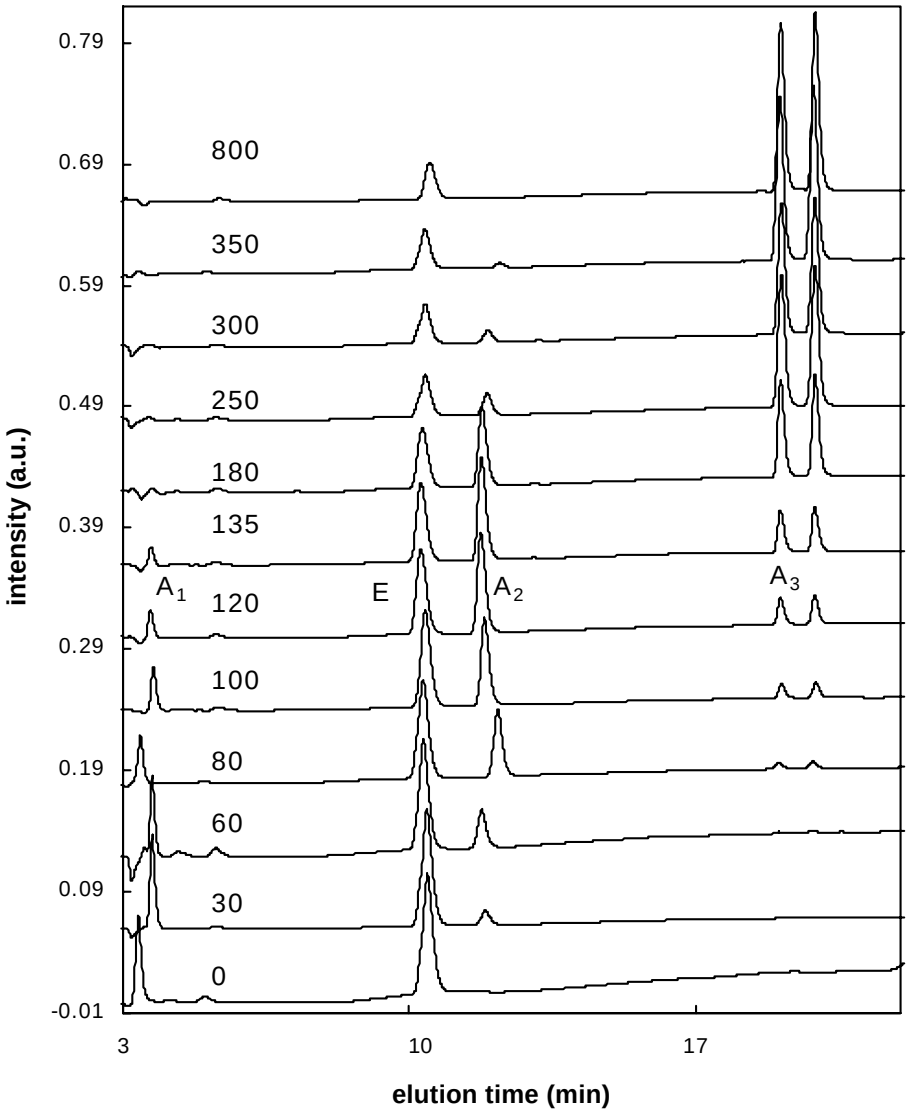

Fig. 1. Overlay of HPLC chromatograms for a PGE + aniline mixture of composition $r = 0.7$ partially cured at 100 °C (cure times in minutes indicated) shifted vertically for clarity; wavelength = 205 nm.

achieve a high sensitivity: 205 nm for the amines and 217 nm for the epoxy. These were used to calculate their concentrations during reaction. Additional proof of the assignment of peaks at different retention times was gained from the coupled HPLC-MAS set-up. The correct assignment is important since small changes in the TFA concentration of the water/acetonitrile solvent, for example, can alter all retention times significantly and even flip those for the epoxy and secondary amine peak.

Calibration curves for the reagents (PGE + aniline) and the synthesized secondary and tertiary amines were constructed over the concentration range of interest for each component in the reactive mixture. A linear dependency was found between the integrated peak of the HPLC chromatogram and the concentrations of these components in the mobile phase.

Concentration profiles for the reaction of PGE + aniline at 100 °C with three different mixture compositions will be given in Section 3.3.2. The reproducibility for calculating the concentration in these cure conditions has been checked by using the same mixture cured in different sample pans and by using different, fresh, reactive mixtures. On average the standard deviation for PGE, aniline, A_2 and A_3 is ±5, ±8, ±5 and ±4%, respectively. The concentration profiles obtained for the stoichiometric mixture at 100 °C by Mijovic et al. with HPLC correspond well to our profiles within these error levels [15].

3.2.2. Validation of the MTDSC signals

3.2.2.1. Link between the heat flow and the consumption rates of reactive groups. The heat flow signal normalized against sample weight (in $W\,g^{-1}$) can be calculated with the production rates of the reactive groups, as defined in the reaction mechanism, and their enthalpies of formation ($\Delta_f H_i^\circ$ in $kJ\,mol^{-1}$):

$$\frac{d_r H^\circ}{dt} = \sum_{i=1}^{N} \frac{d[B_i]}{dt} \Delta_f H_i^\circ \tag{1}$$

with $d[B_i]/dt$ the production rate (− sign for reagents, + sign for products) in $mol\,kg^{-1}\,s^{-1}$ and $[B_i]$ the concentration of component B_i in $mol\,kg^{-1}$, respectively; superscript (°) denotes thermodynamic quantities in their standard states (1 atm) and N the number of substances involved in the reactions.

An equal reaction enthalpy was found for the primary amine and secondary amine–epoxy reaction steps [41]. This means that the heat flow signal can be directly calculated from the conversion (x) rate of epoxide groups:

$$\frac{d_r H}{dt} = \frac{dx}{dt} \Delta_r H, \quad \text{with } x(t) = \frac{[E]_0 - [E]}{[E]_0} \tag{2}$$

or by integration to time t:

$$\Delta_r H(t) = x(t)\, \Delta_r H \tag{3}$$

with $[E]_0$ and $[E]$ the concentration of epoxide groups at time 0 and at time t, respectively; $\Delta_r H$ is the reaction enthalpy (superscript (°) is omitted). Note that $\Delta_r H$ corresponds to the reaction exothermicity when all epoxide groups are converted, while $\Delta_r H(t)$ designates the partial reaction exothermicity till time t. The effect of cure temperature on this value is negligible [41]. The constant ratio between the heat release and the epoxy conversion can be directly inferred by comparing the epoxy conversion obtained from chromatography with the running integral of the heat flow during isothermal PGE + aniline reaction as depicted in Fig. 2. The agreement with an average constant ratio is clear for all mixture compositions, signifying that both amine–epoxy reactions have the same or a similar contribution to the reaction enthalpy throughout the reaction path. In the case of a different contribution, a certain curvature would be present, which would be enhanced by changing the mixture composition due to a change in the contribution of both reaction steps.

3.2.2.2. Reaction heat capacity in relation to the concentration profiles. When the heat capacities of reagents and products ($C_{p,i}$ in $J\,mol^{-1}\,K^{-1}$) are known, the reaction heat capacity can be calculated (in $J\,kg^{-1}\,K^{-1}$):

$$\Delta_r C_p = \sum_{i=1}^{N} [B_i] C_{p,i} \tag{4}$$

where $[B_i]$ (in $mol\,kg^{-1}$) has to be preceded by the correct sign: + for products and − for reagents. To estimate the reaction heat capacity, an additivity approach based on a nearest-neighbor approximation will be used. A molecular property is considered to be composed of contributions due to groups, which are defined as polyvalent atoms (ligancy ≥2) in a molecule together with all their ligands. Using the accepted nomenclature, C–(H)$_3$(C) represents a C atom connected to three H atoms and another C atom, that is, an alkyl group. Group contributions were introduced by Benson and Buss to estimate the heat capacity (C_p°), entropy (S°) and enthalpy of formation ($\Delta_f H^\circ$) for ideal gases at 298.15 K and 1 atm [47]. When more data on heat capacities in the liquid state became available, their group contributions were published [48]. A more recent article has further extended the applicability of the additivity method by including C–H–N–O–S–halogen compounds in the gas, liquid and solid states at 298.15 K [49]. When using this group additivity approach to calculate $\Delta_r C_p$ for PGE + aniline, only those groups that change during the reaction have to be considered. The reaction heat capacities of the primary amine–epoxy and secondary amine–epoxy reaction steps can be calculated using values at 298.15 K from [49], corrected with a new value of the group N–(H)(C)(CB)

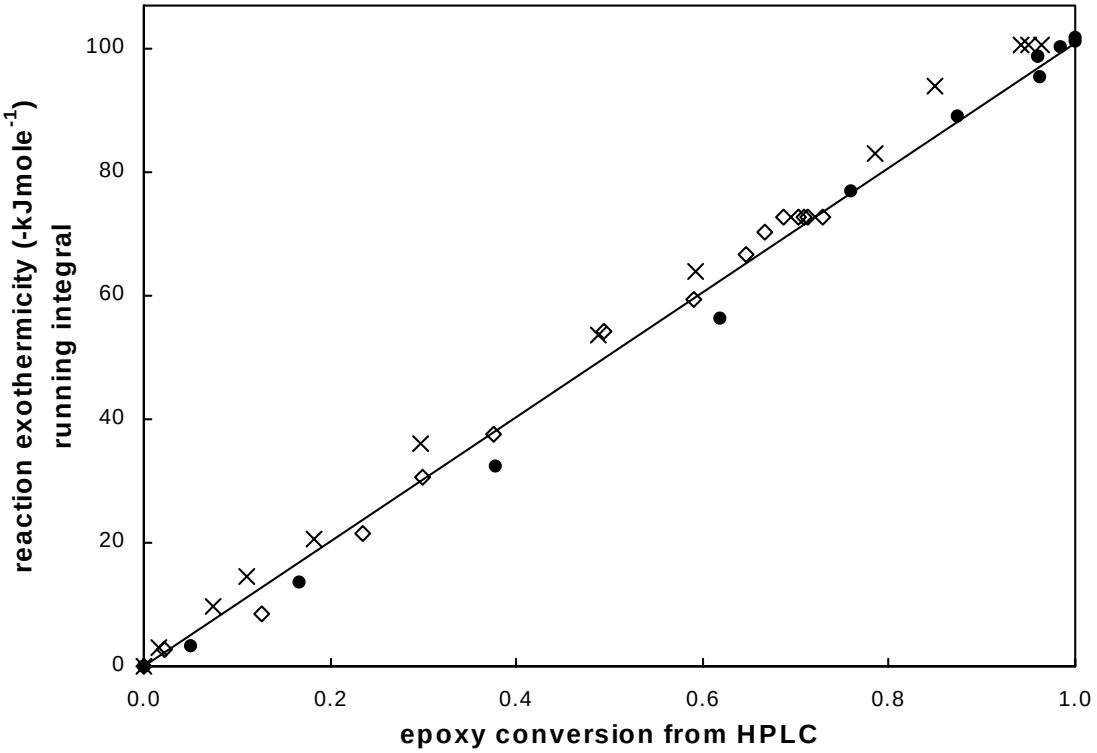

Fig. 2. Running integral of the reaction exothermicity from MTDSC (normalized per mole epoxy) during isothermal cure of PGE + aniline at 100 °C as a function of the epoxy conversion obtained from HPLC with mixture compositions (r) of 0.7 (◇), 1.0 (×) and 1.39 (●); a constant ratio is depicted (—).

[41] and accounting for the effect of cure temperature [41]:

$$\begin{aligned}\Delta_r C_{p,\text{prim}} &= 16.1 + 0.018(T_{\text{cure}} - 298.15) \\ &\quad - 0.00085(T_{\text{cure}} - 298.15)^2 \\ \Delta_r C_{p,\text{sec}} &= 12.6 + 0.35(T_{\text{cure}} - 298.15) \\ &\quad - 0.00024(T_{\text{cure}} - 298.15)^2\end{aligned} \tag{5}$$

with T_{cure} in K.

Thus, both reaction steps contribute differently to the reaction heat capacity, especially at higher cure temperatures. The difference can be illustrated by comparing $\Delta_r C_p$ as measured by MTDSC at certain cure times with the epoxy conversion from HPLC. Two systems are overlaid in Fig. 3, namely PGE + aniline ($r = 1$), in which both primary and secondary amines react with the epoxy and PGE + A_2 ($r = 1$), for which only the secondary amine reaction occurs. Both were reacted at 100 °C. The latter $\Delta_r C_p$ indeed increases linearly with conversion, while the former shows a slower increase till around 60% conversion, corresponding to a smaller contribution from $\Delta_r C_{p,\text{prim}}$ as can be seen in Eq. (5). Since the secondary amine–epoxy reaction becomes dominant from around 70% conversion in the PGE + aniline reaction (see also discussion of Fig. 7), the tangent in these final stages is parallel to the one corresponding to the PGE + A_2 reaction (indicated in Fig. 3).

The quantification of heat capacity changes at different temperatures and mixture compositions will be implemented by Eq. (5) combined with the corresponding concentration profiles from the amine–epoxy reaction step obtained from the kinetic model (see also Eq. (4)):

$$\Delta_r C_p = \Delta_r C_{p,\text{prim}}([A_2] + [A_3]) + \Delta_r C_{p,\text{sec}}[A_3] \tag{6}$$

Both $\Delta_r C_{p,\text{prim}}$ and $\Delta_r C_{p,\text{sec}}$ as a function of T_{cure} (Eq. (5)) were optimized [41] in a wide range of PGE + aniline/A_2 mixture compositions and cure temperatures. Although fine-tuning of these equations is possible as an optimization strategy, focus will be on optimizing the kinetic parameters.

3.3. Kinetics of the epoxy–amine reaction

3.3.1. Initial reaction rates and validity of the proposed reaction mechanism

In order to obtain a meaningful start set of kinetic parameters and thus improve the reliability of the optimized set, some of these parameters will be determined independently first. By combining the systems PGE + aniline and PGE + A_2, both the initial reaction rate and the intermediate stages of the former system can be determined. Note that the non-reactive complexes will not be considered in calculating the initial reaction rates.

3.3.1.1. Effect of composition. The consumption rate of epoxide groups at $t = 0$ for PGE + aniline evolves with

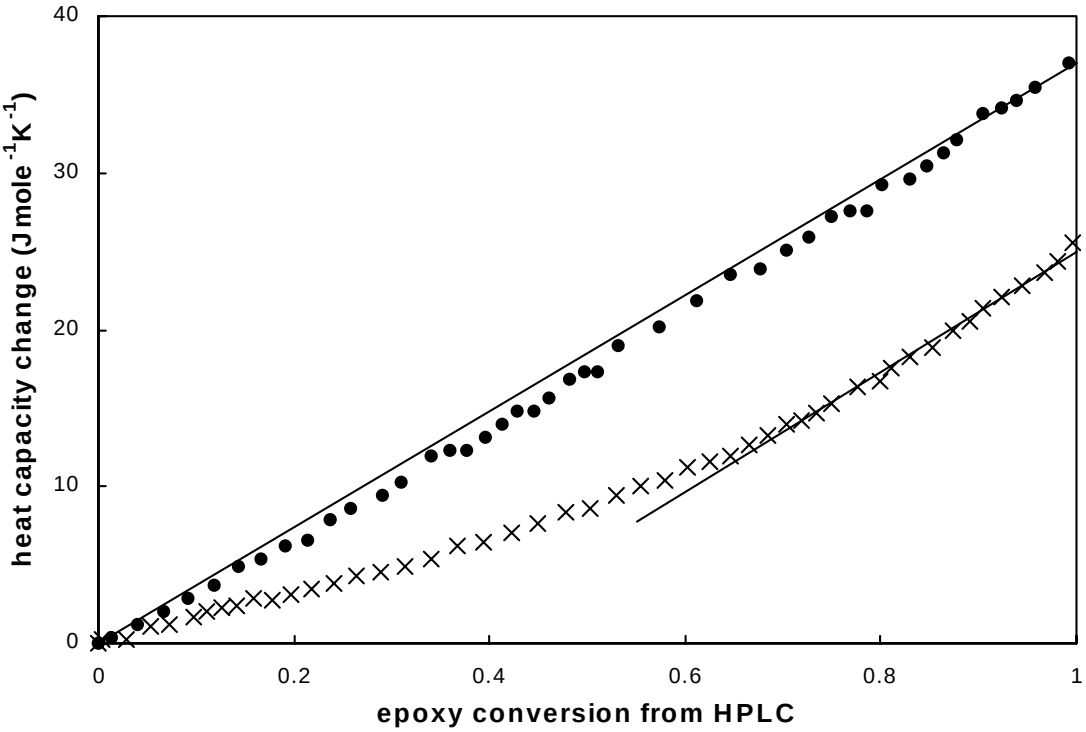

Fig. 3. Heat capacity change (normalized per mole epoxy) during isothermal cure of PGE + aniline ($r = 1$) (×) and PGE + A_2 ($r = 1$) (●) at 100 °C as a function of the epoxy conversion obtained from HPLC measurements.

second order in the initial primary amine concentration as can be calculated from the reaction mechanism in Scheme 1:

$$-\left.\frac{\mathrm{d[E]}}{\mathrm{d}t}\right|_0 = k_{1A1}[EA_1]_0[A_1]_0 = k'_{1A1}[E]_0[A_1]_0^2 \quad \text{(for PGE + aniline)} \tag{7}$$

According to Eq. (2) and by using the heat flow at $t = 0$ (see Fig. 4), the initial conversion rate can be calculated:

$$-\left.\frac{\mathrm{d[E]}}{\mathrm{d}t}\right|_0 \frac{1}{[E]_0} = \left.\frac{\mathrm{d}x}{\mathrm{d}t}\right|_0 = \left.\frac{\mathrm{d}_r H}{\mathrm{d}t}\right|_0 \frac{1}{\Delta_r H} \tag{8}$$

The reaction enthalpy $\Delta_r H$ corresponds to the total reaction exothermicity per mole of epoxide groups equaling $-99\,\mathrm{kJ\,mol^{-1}}$ on average for stoichiometric and excess amine mixtures. This value is also used for PGE + aniline mixtures having an excess of epoxide groups, resulting in final conversions smaller than 1. Fig. 5 plots the initial conversion rate as a function of the initial concentration of aniline corresponding to a quadratic dependence (slope in a log–log scale equals 2). The value for k'_{1A1} at 100 °C from this fit is $3.9 \times 10^{-6}\,\mathrm{kg^2\,s^{-1}\,mol^{-2}}$. Thus, Eq. (7) can correctly describe the initial rate of this system. The rate of the uncatalyzed reaction step, consisting of the reaction of E with A_1 without an equilibrium complex, is therefore negligible as confirmed by other workers [20,23,24].

Since the model compound A_2 initially contains hydroxyl groups with a concentration equal to that of the secondary amine functionalities, $[OH]_0 = [A_2]_0$, the initial rate of the PGE + A_2 system corresponds to the secondary amine–epoxy reaction catalyzed by hydroxyl groups:

$$-\left.\frac{\mathrm{d[E]}}{\mathrm{d}t}\right|_0 = k_{2OH}[EOH]_0[A_2]_0 = k'_{2OH}[E]_0[OH]_0[A_2]_0 \quad \text{(for PGE + } A_2\text{)} \tag{9}$$

No acceleration is seen during the PGE + A_2 reaction at 100 °C in Fig. 4, meaning that the depletion of secondary amine groups is more important than the further increase in OH concentration. Note the high initial reaction rate of this system in comparison to PGE + aniline, in which the autocatalytic behavior is clearly present at the same reaction temperature, expressing the strong catalytic influence of OH groups. The heat flow does not seem to be a reliable candidate to determine the initial reaction rate for the PGE + A_2 system since part of the reaction will already take place in the temperature ramp towards the reaction temperature. The measured heat flow at $t = 0$ will therefore be an underestimation of the initial reaction rate. However, since the heat capacity signal corresponds to the evolution in conversion in this system (see Fig. 3), the initial reaction rate can be obtained from its slope as indicated in Fig. 4. After normalization of this signal to a conversion profile, k'_{2OH} was calculated from Eq. (9) to be $(4.0 \times 10^{-5} \pm 0.3 \times 10^{-5})\,\mathrm{kg^2\,s^{-1}\,mol^{-2}}$ at 100 °C for an initial A_2 concentration ranging from 2 to $3\,\mathrm{mol\,kg^{-1}}$, proving the validity of

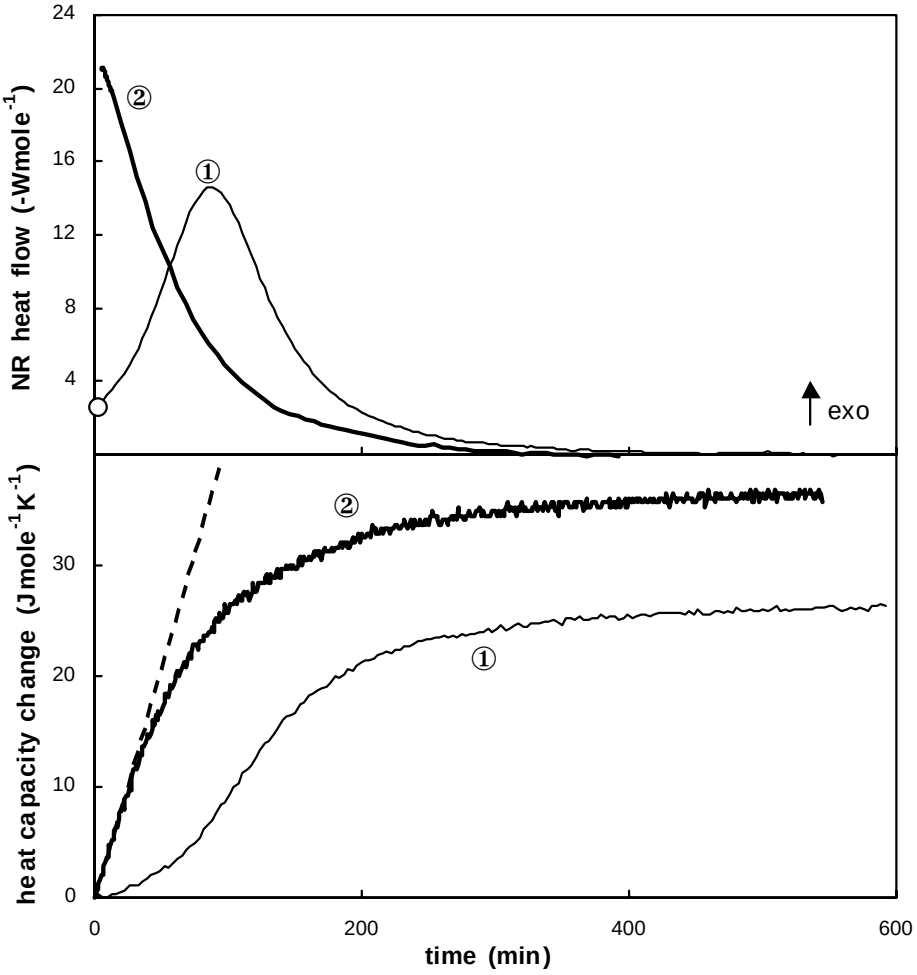

Fig. 4. Non-reversing (NR) heat flow and heat capacity change for the reaction of stoichiometric mixtures of PGE + aniline (thin line) and PGE + A_2 (thick line) at 100 °C; the initial reaction rate was calculated using the heat flow (○) and heat capacity signal (- - -) for PGE + aniline and PGE + A_2, respectively (see text).

Eq. (9). The uncatalyzed reaction between A_2 and E or that with transition complexes like EA_1 and EA_2 is thus negligible as confirmed by Mijovic et al. on the same system [15].

3.3.1.2. Effect of reaction temperature. Using Eqs. (7) and (9) together with the aforementioned experimental approach based on the heat flow and heat capacity signals, the initial reaction rates can be calculated as a function of temperature for PGE + aniline (from 70 to 130 °C) and PGE + A_2 (from 70 to 90 °C), respectively. The upper temperature limit is lower for the latter system, due to its higher reaction rate.

The Arrhenius dependencies from Fig. 6 show activation energies of 77.3 and 43.6 kJ mol^{-1} for the amine catalyzed primary amine–epoxy reaction (E'_{1A1}) and for the hydroxyl catalyzed secondary amine–epoxy reaction (E'_{2OH}), respectively. These values will be used as initial parameters for the optimization program FITME.

3.3.1.3. Absence of side reactions. Additional experiments were performed to confirm the information in literature about the absence of side reactions such as etherification and homopolymerization in the PGE + aniline system [11,19]. Firstly, the relationship between reaction enthalpy and mixture composition has been shown to be constant and equal to −99 kJ mol^{-1} of minority component [20,41]. If one or both side reactions would take place, a higher reaction enthalpy would be found for mixtures with an excess of epoxide groups. Secondly, non-isothermal MTDSC experiments were performed on mixtures of PGE with (i) a small amount of aniline (large epoxy excess), (ii) the tertiary amine *N*,*N*-bis(3-phenoxy-2-hydroxypropyl)aniline (A_3). No reaction can be detected for these mixtures until 230 °C, from where degradation starts to occur. The lack of efficiency with which the tertiary amine A_3 induces side reactions can be attributed to steric factors [50]. In case of aliphatic amines, for example, higher efficiencies were found [18].

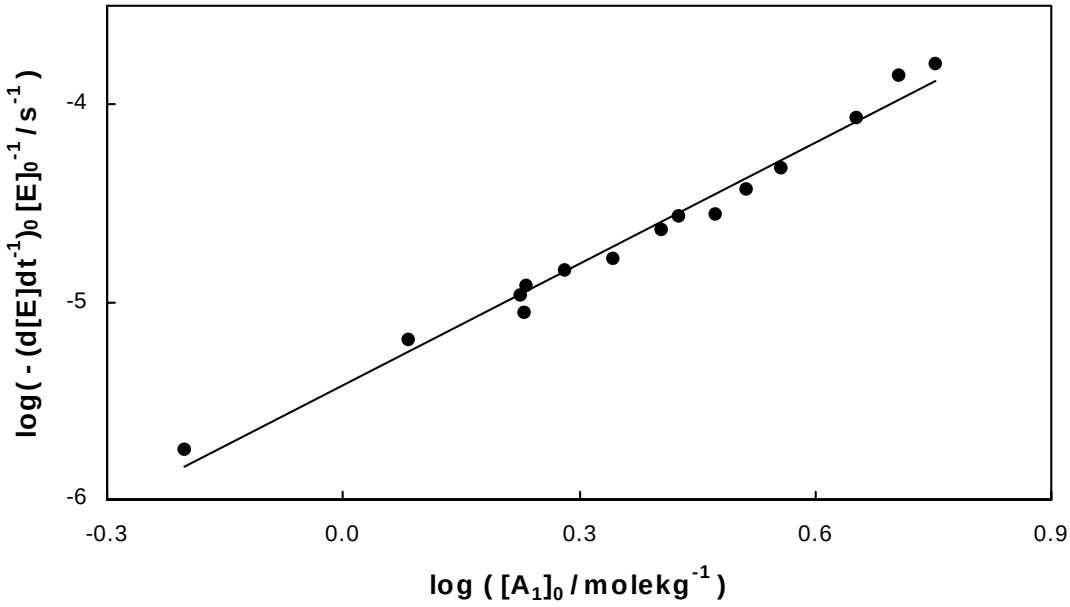

Fig. 5. The conversion rate of epoxide groups at $t = 0$ and 100 °C as calculated from the non-reversing heat flow signal as a function of the initial concentration of primary amine groups (●) (log–log scale); best fit with second order rate equation in $[A_1]_0$: $k'_{1A1} = 3.9 \times 10^{-6}\,kg^2\,s^{-1}\,mol^{-2}$ (—).

3.3.2. Optimization of the reaction mechanism

3.3.2.1. Modeling strategy. To optimize the kinetic parameters and equilibrium constants of the reaction mechanism of Scheme 1, non-reversing heat flow and heat capacity signals from MTDSC experiments will be used. The latter will be introduced here for the first time as a quantitative tool for reaction kinetics modeling since it has been shown [41] to be a candidate to distinguish between primary amine and secondary amine–epoxy reaction steps. The effect of cure temperature is included by combining non-isothermal experiments with heating rates from 1 to 2.5 °C min^{-1} with isothermal experiments from 70 to 120 °C. Isothermal cure experiments have the obvious advantage of uncoupling the

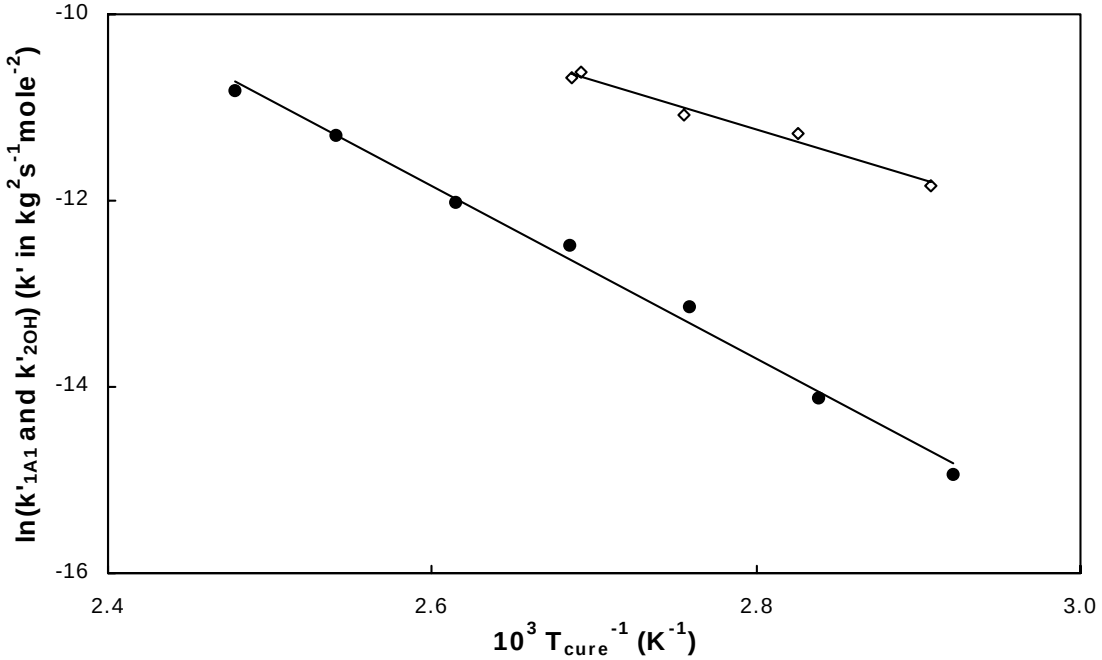

Fig. 6. Arrhenius plots of the rate constants k'_{1A1} and k'_{2OH} as calculated from the non-reversing heat flow and normalized heat capacity signals, respectively: $\ln k'_{1A1}$ (●) and $\ln k'_{2OH}$ (◇); results of linear regression curves (—): $E'_{1A1} = 77.3\,kJ\,mol^{-1}$, $\ln A'_{1A1} = 12.3$ with $R^2 = 0.99$ and $E'_{2OH} = 43.6\,kJ\,mol^{-1}$, $\ln A'_{2OH} = 3.5$ with $R^2 = 0.98$.

variables of temperature and time. Mixture compositions (r = mole NH/mole oxirane) range from 0.6 to 5 and correspond to initial concentrations of PGE and aniline of $[A_1]_0 = 1.68$; $[E]_0 = 5.62\,mol\,kg^{-1}$ and $[A_1]_0 = 6.53$; $[E]_0 = 2.61\,mol\,kg^{-1}$, respectively.

Equilibrium constants for complex formation were obtained for different model compounds—containing hydroxyl, amine, epoxy and ether groups—by spectroscopic and calorimetric measurements [20,23,26]. While methodological difficulties restrict the measurement of these constants at higher temperatures, these results indicate a decrease in the equilibrium constant with increasing temperature. The equilibrium constant of the epoxy–hydroxyl complex (K_{EOH}), for example, equals 1.43 ($kg\,mol^{-1}$) at 22 °C and 0.51 ($kg\,mol^{-1}$) at 97 °C [20]. This corresponds to a difference in activation energy of $12.5\,kJ\,mol^{-1}$ between the dissociation and formation of this complex. A recent study used a simple mechanistic model for DGEBA + ethylenediamine where different isothermal and non-isothermal DSC measurements could be optimized when K_{EOH} was allowed to decrease with cure temperature [51]. Another study in which a more complex mechanistic model was optimized for PGE + aniline, including most reactive and non-reactive complexes (see also Table 2), did not include this temperature dependency in order to reduce the number of model parameters [16]. The temperature effect on the equilibrium constants can be easily implemented in the optimization methodology of FITME by allowing a difference in the activation energies of formation and dissociation of complexes. This has been attempted for the reactive complexes EOH and EA1, but no satisfactory optimum could be obtained in this way. The non-reactive complexes, as presented in the mechanistic model of Scheme 1, have to be included to achieve an optimum set, as will be illustrated further on. Since no temperature dependence has to be assumed in this case (both non-reactive and reactive complexes included) and since no direct experimental information on the thermodynamics of complexes ($\Delta_f H^\circ$) and their temperature dependence was gathered in this work, these effects will not be implemented. In view of the experimental cure temperature range, the literature values for equilibrium constants around 100 °C will be used as initial values [20,23,26].

The pre-exponential factors and activation energies presented in the previous sections in case of k'_{1A1} ($=k_{1A1}K_{EA1}$) and k'_{2OH} ($=k_{2OH}K_{EOH}$) can be used to obtain an initial parameter set for the rate constants. Finally, to obtain initial A_{1OH} and E_{1OH} values, the ratio k_{2OH}/k_{1OH} was assumed to equal 0.5. In addition to the reaction mechanism of Scheme 1, other reaction steps were initially included in the kinetic mechanism: uncatalyzed primary amine and secondary amine–epoxy reactions and the secondary amine–epoxy reaction catalyzed by primary amine. Both were found, however, to have rate constants more than two orders of magnitude smaller than that of the primary amine–epoxy reaction catalyzed by the primary amine (k_{1A1}).

3.3.2.2. Optimized kinetic parameter set. Optimization consists of the simultaneous treatment of all isothermal and non-isothermal experiments using different mixture compositions. The optimized parameter set, corresponding to the least sum of squares between simulated and experimental data, is given in Table 1. Using these parameters, rate constants at different temperatures can be calculated. At 100 °C, for example, k_{1A1}, k_{1OH} and k_{2OH} equal 8.95×10^{-5}, 2.18×10^{-3} and $3.93 \times 10^{-4}\,kg\,mol^{-1}\,s^{-1}$, respectively. Note that the optimized equilibrium constants are within the range found in the literature (from 0.1 to $1\,kg\,mol^{-1}$) [20,23,26].

In agreement with other studies [11,16,26], the primary amine–epoxy reaction catalyzed by primary amines is over one order of magnitude slower, in the range of cure temperatures of interest, as compared to the one catalyzed by hydroxyl groups. The consumption rates of epoxide groups for the three major reaction steps are compared in Fig. 7. This graph clearly shows the need for step (1A1) in initiating the epoxy–amine reaction, while the hydroxyl catalysis (1OH) takes over after the initial stages of reaction (2% epoxy conversion at 100 °C). A competition between the primary amine and secondary amine for reaction with epoxy functionalities takes place from around 50% epoxy conversion (at 100 °C), indicating that the consumption of the primary amine groups, reducing the rate of this step, counteracts its higher reaction rate constant (k_{1OH}).

3.3.2.3. Comments on the proposed model. While the simulation capability of the optimized model will be elaborated in Section 3.4 for a wide range of cure temperatures and mixture compositions, the reaction of a stoichiometric PGE + aniline mixture at 100 °C will be used here to illustrate the relevance of the different reaction steps in the mechanism

Table 1
Optimized kinetic and equilibrium parameters for the reaction of PGE + aniline using Scheme 1; activation energies (E) are in $kJ\,mol^{-1}$; pre-exponential factors (A) are in $kg\,mol^{-1}\,s^{-1}$

Kinetic parameters ($kg\,mol^{-1}\,s^{-1}$)						Equilibrium constants ($kg\,mol^{-1}$)				
k_{1A1}		k_{1OH}		k_{2OH}		K_{EOH}	K_{A1OH}	K_{EA1}	K_{EtOH}	K_{EtA1}
E_{1A1}	$\log A_{1A1}$	E_{1OH}	$\log A_{1OH}$	E_{2OH}	$\log A_{2OH}$					
72.3	6.1	50.4	4.4	52.2	3.9	0.36	0.22	0.28	0.22	0.22

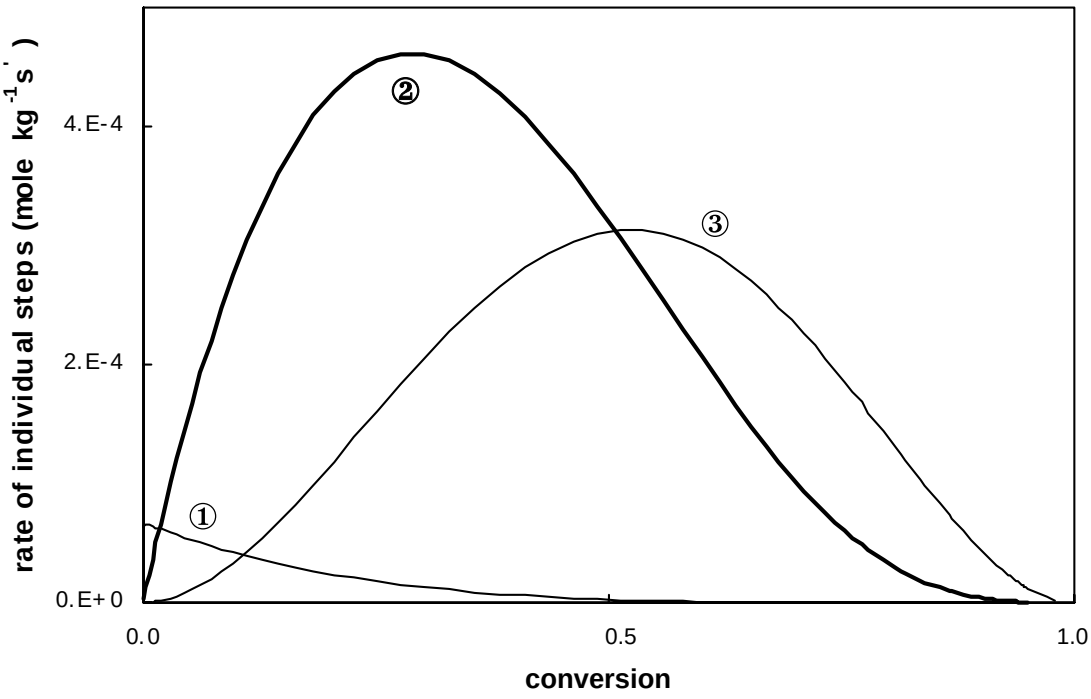

Fig. 7. Comparison between the rates of the three most important reaction steps: primary amine with the epoxy–amine complex (① : 1A1); primary amine with the epoxy–hydroxyl complex (② : 1OH) and secondary amine with the epoxy–hydroxyl complex (③ : 2OH) for a stoichiometric PGE + aniline mixture at 100 °C.

of Scheme 1. The prediction of the experimental trends obtained from MTDSC and HPLC, using the optimized set of parameters from Table 1, are shown as thick lines in Figs. 8 and 9.

When a reaction mechanism is used without equilibrium complexes (based on Scheme 2), it is not possible to achieve an optimized parameter set that can predict both the non-reversing heat flow and the heat capacity signal or the concentration trends obtained from HPLC simultaneously (see also Table 2, discussed in the next section). Optimization of the kinetic parameters of this model in order to obtain a good prediction of the non-reversing heat flow (case (i) in Table 2), for example, results in a poor simulation of, especially, the A_2 concentration profile (Fig. 8). This can be ascribed to an incorrect substitution effect as will be discussed in the next section.

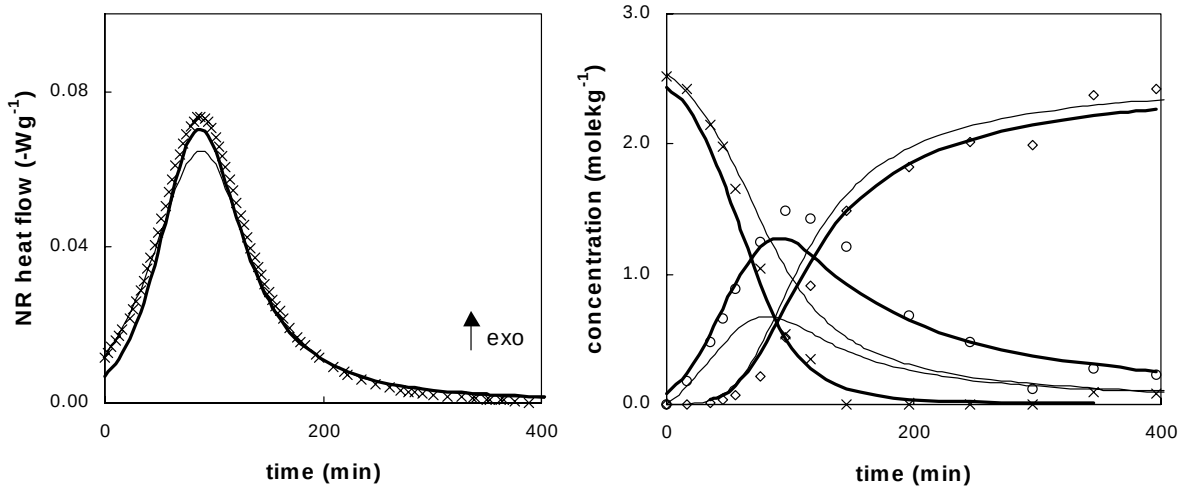

Fig. 8. Non-reversing (NR) heat flow from MTDSC (×) and concentration profiles from HPLC (aniline [A_1] (×), the secondary amine [A_2] (○) and the tertiary amine [A_3] (◇)) for a stoichiometric PGE + aniline mixture cured at 100 °C; simulation using the parameter set of Table 1 (thick line), corresponding to the reaction mechanism of Scheme 1; simulation using the parameter set of case (i) in Table 2 (thin line).

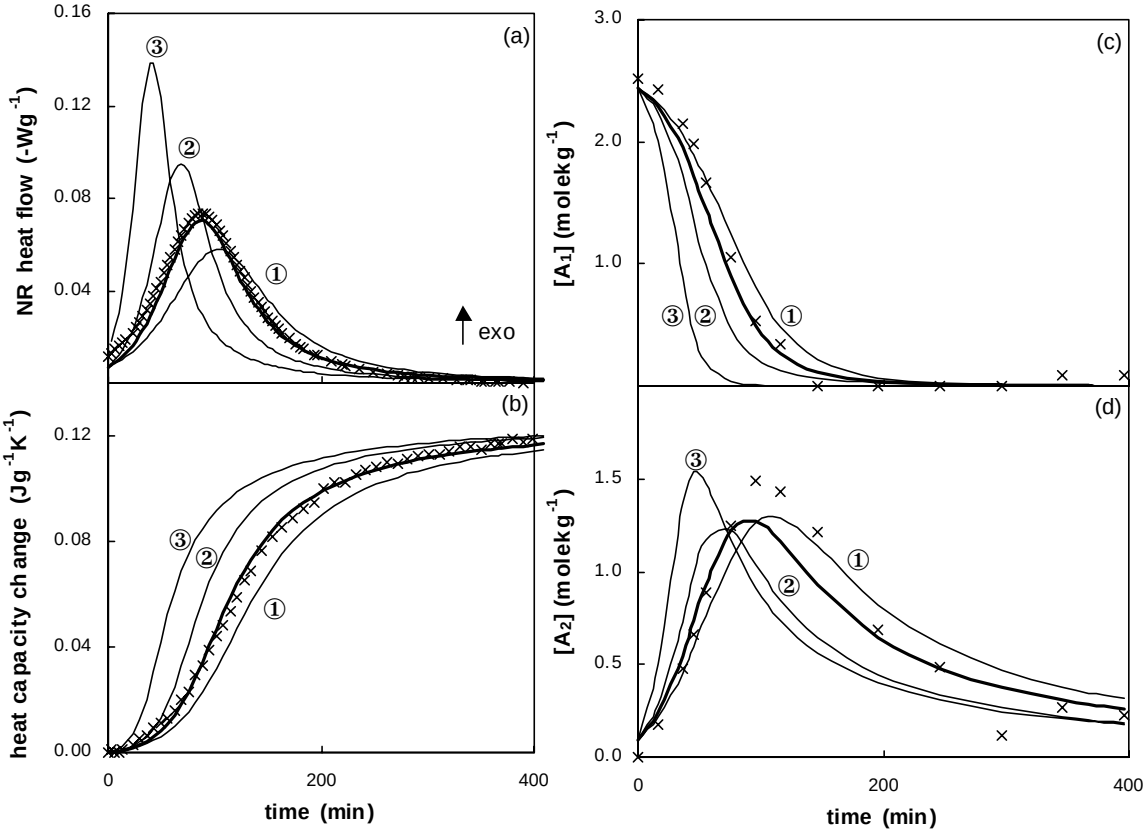

Fig. 9. Non-reversing (NR) heat flow (a) and heat capacity change (b) from MTDSC and concentration profiles from HPLC (aniline [A_1] (c), the secondary amine [A_2] (d)) for a stoichiometric PGE + aniline mixture cured at 100 °C; experimental points (×); simulations using the parameter set of Table 1 (thick line), corresponding to the reaction mechanism of Scheme 1; simulations using the same reaction mechanism and parameter set, while changing the equilibrium constants of the non-reactive complexes: $K_{EtOH} = 0.44$ (①), $K_{EtOH} = 0$ (②) and $K_{EtOH} = K_{A1OH} = K_{EtA1} = 0$ (③) (thin lines).

Thus, the reaction mechanism of Scheme 1 (including equilibrium complexes) with the optimized parameter set of Table 1 is needed to achieve an adequate simulation capability.

Deviations from the optimum values of the equilibrium constants for the non-reactive complexes illustrate the significance of these complexes in the mechanism (Fig. 9). When the equilibrium constant of the ether–hydroxyl interaction is increased (K_{EtOH} doubled in ①), for example, the increase of reaction rate due to autocatalysis is clearly postponed, resulting in a delay of the heat flow maximum and of the other profiles depicted in Fig. 9. On the other hand, assuming that the EtOH complex is absent (②) or omitting non-reactive complexes altogether (③), results in impermissible, simulated rises in reaction rate. Note that the higher maximum in the simulated concentration profile of A_2 in this last case relates to the higher amount of A_1 groups available for reaction (since $K_{A1OH} = K_{EtA1} = 0$).

3.3.2.4. Comparison with literature. Mechanistic studies on PGE + aniline as presented in the literature are included in Table 2 with their kinetic parameters and activation energies. To compare studies with and without complexes, all rate constants were expressed for the pseudo-trimolecular amine–epoxy reaction as introduced in Section 3.1 (k'). However, due to the use of reaction mechanisms with different reaction steps and, when included, different complexes, these values cannot be strictly compared.

The substitution effect is calculated by taking the ratio of consumption rates of epoxide groups by primary and secondary amine functionalities, termed reactivity ratio (see Scheme 1): $k_{2OH}[EOH]/(k_{1OH}[EOH] + k_{1A1}[EA_1])$. For the PGE + aniline system, an average negative substitution effect of 0.2 is found in this way, over the entire conversion range and in the experimental range from 70 to 120 °C. Thus, PGE + aniline is characterized by a negative substitution effect, which is in agreement with some literature values but in disagreement with others (summarized in Table 2). As indicated in the introduction, the values of k_{2OH}/k_{1OH} or k'_{2OH}/k'_{1OH} should be used with care to compare reactivity ratios since different reaction mechanisms cannot be compared in this way. Since k_{1A1} was found to be small in comparison to k_{1OH} and k_{2OH}, the reactivity ratio does correspond to k_{2OH}/k_{1OH} in this work.

While some studies investigated the effect of cure temperature for stoichiometric mixtures, others varied the mixture

Table 2
Literature results on kinetic rate constants and equilibrium constants for PGE + aniline compared to those of Scheme 1 (this work): the notation as introduced in Section 3.1 is used to identify rate constants with (k) or without the explicit use of complexes (k')

System and mechanism (rate/equilibrium constants)	Technique	T_{cure} (i and n-i) and mixtures (°C/°C min^{-1} and r = NH/E)	Rate constants (at 100 °C[0]) $K_{EA1}k_{1A1}/K_{EOH}k_{1OH}/K_{2OH}k_{2OH}$ (kg^2 mol^{-2} s^{-1})	Reactivity ratio	Activation energy $E_{1A1}/E_{1OH}/E_{2OH}$ (kJ mol^{-1})
Optimized parameters: LSSQ					
PGE + aniline	MTDSC: HF&Cp	i70–120/n-i@1 − 2.5	2.52E−5/7.75E−4/1.39E−4	0.18	72.3/50.4/52.2
$k_{1A1,iOH}$/		r = 0.6–5	1.22E−4/2.32E−3/4.34E−4	0.19	
$K_{EA1,A1OH,EOH,EtA1,EtOH}$			(at 127 °C)	(at 127 °C)	
				k_{2OH}/k_{1OH}	
Literature results					
PGE + aniline [16]	DSC	i127	2.56E−4/1.27E−3/2.11E−3	1.66	na
$k_{1A1,iOH,iOHOH}$/		r = 0.5–5	At 127 °C	At 127 °C	
$K_{EA1,EOH,A1OH,A2OH}$					
PGE + aniline[1] [26]	Calorimetry	i60–90	6.32E−6/5.75E−5/1.60E−5[2]	0.28	46/39/41
$k_{1A1,2A2,iOH}/K_{EOH,AiOH}$		r = 1–10			
PGE + aniline[1] [23]	Calorimetry and IR	i90–130	8.43E−6/6.48E−5/8.70E−6[2]	0.13	46/39/41
$k_{1A1,2A2,iOH}/K_{EOH,AiOH}$		r = 1–10			
			$k'_{1A1}/k'_{1OH}/k'_{2OH}$ (kg^2 mol^{-2} s^{-1})	k'_{2OH}/k'_{1OH}	$E'_{1A1}/E'_{1OH}/E'_{2OH}$ (kJ mol^{-1})
Optimized parameters with restricted simulation capability (only in stated T_{cure} and r range)					
Case i	MTDSC:HF	i70–120/n-i@1–2.5	3.83E−6/3.92E−5/8.12E−5	2.07	77.2/51.4/48.6
PGE + aniline		r = 0.6–1.4			
$k'_{1A1,iOH}$					
Case ii	MTDSC:HF&Cp	i80–100	2.52E−6/7.41E−5/4.32E−5	0.58	77.2/55.3/56.5
PGE + aniline		r = 1.4–5			
$k'_{1A1,iOH}$					
Case iii	HPLC	i100	2.52E−6/6.18E−5/3.39E−5	0.55	77.2/51.4/48.6[3]
PGE + aniline		r = 0.7–1.4			
$k'_{1A1,iOH}$					
Literature results					
PGE + aniline [11]	Near-IR	i100–160	1.92E−6/4.72E−5/2.84E−5	0.60	80/45/44
$k'_{1A1,iOH}$		r = 1			
PGE + aniline [15]	HPLC	i90–120	na/1.09E−4/2.28E−5	0.21	na/54/33
k'_{iHX}[4]$_{,iOH,iOHOH}$		r = 1			
PGE + aniline [13]	HPLC	i75	na	0.30[5]	na
k'_{iu}		r = 0.7–1.7			
PGE + *m*PDA[6] [11]	Near-IR	i100–160	7.10E−6/8.52E−5/4.37E−5	0.51	46/28/33
$k'_{1A1,iOH}$		r = 1			
PGE + NMA[7] [25]	Near-IR	i110–170	na/na/3.63E−5	na	na/na/55
$k'_{2A2,2OH}$		r = 1			

Other approaches (without the introduction of complexes) are also included (discussed in text); i: isothermal; n-i: non-isothermal; @: heating rate; [0]unless stated otherwise; [1]performed in *o*-dichlorobenzene; [2]k_{2OH} was determined from the model PGE reaction with *N*-ethylaniline; [3]activation energies taken from optimization with HF; [4]HX: hydroxyl groups initially present in traces of impurities; [5]k_{u2}/k_{u1}; [6]*m*PDA: *m*-phenylenediamine; [7]NMA: *N*-methylaniline.

composition or both. Also note that one study was performed in *o*-dichlorobenzene, which could have had an effect on the reaction kinetics. Actually, Shechter studied the influence of different solvents and found that compounds with hydroxyl groups had an obvious catalytic effect on the epoxy–amine reaction, while other polar solvents such as acetone and benzene actually had a retarding effect [21]. An inhibition effect has been observed at high conversions for PGE + aniline in *o*-chlorobenzene as solvent. This effect was attributed to the higher basicity of secondary and tertiary amine groups in comparison to that of the primary amine groups [52]. In some conditions, epoxy conversions as low as 60% were found at 90 °C, and were observed to increase with an increase in reaction temperature [23]. No indications for this inhibition effect are present in this work, since reaction enthalpies at all measurable temperatures were close to −100 kJ mol^{-1}. Also note that glass transitions after reaction completion were equal to 9 °C for stoichiometric mixtures measured from 45 to 120 °C. Consequently (partial) vitrification effects were not interfering.

Different approaches are used in the literature to obtain a set of kinetic parameters. Most early studies determined each rate constant separately by developing conditions in which each dominated the reaction rate. For this purpose, different PGE + aniline compositions had to be combined with model compounds for secondary and tertiary amines and

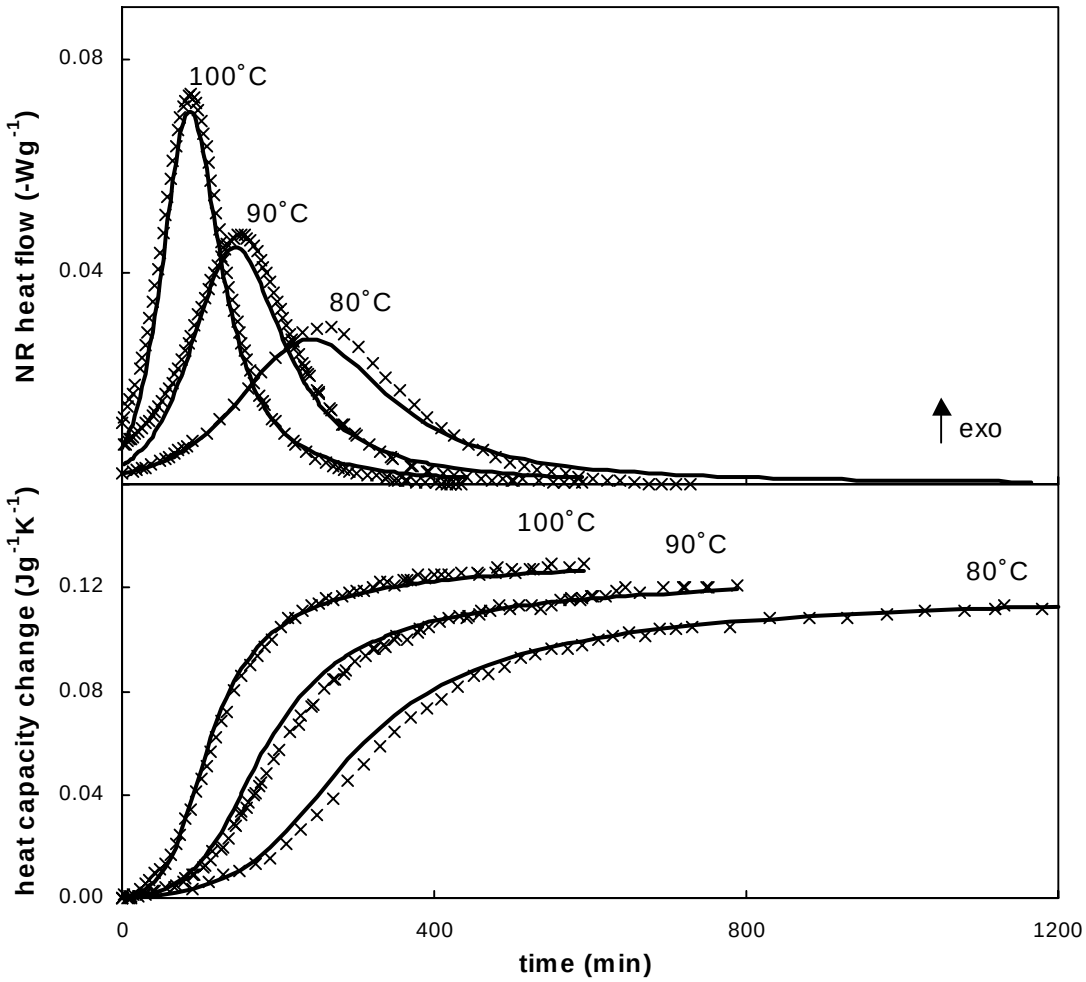

Fig. 10. Non-reversing (NR) heat flow (×) and heat capacity change (×) for the reaction of stoichiometric PGE + aniline mixtures at 80, 90 and 100 °C; simulation using the parameter set of Table 1 (—).

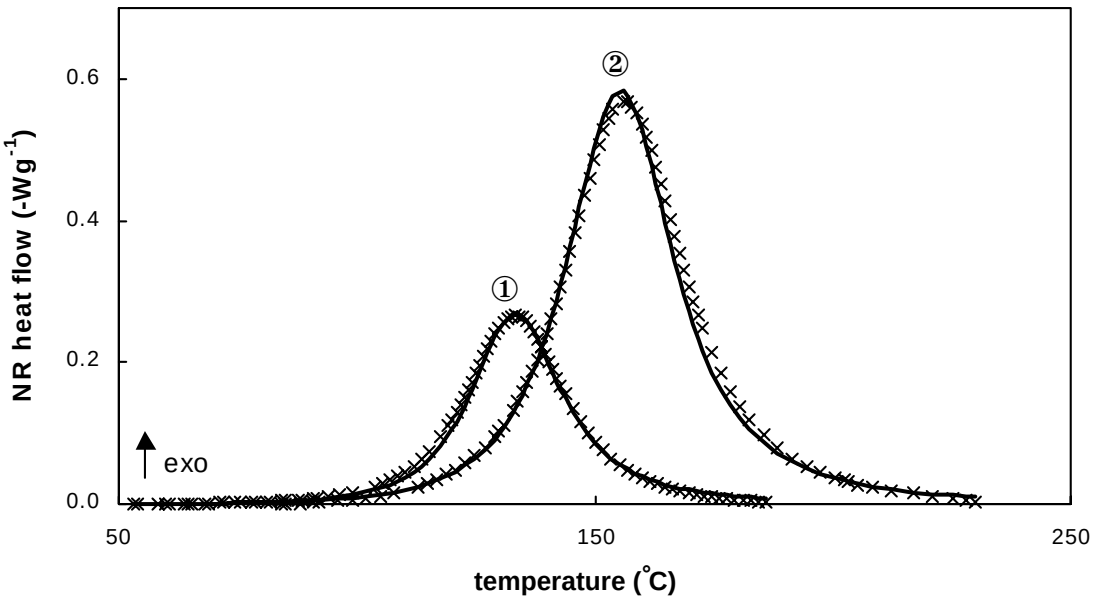

Fig. 11. Non-reversing (NR) heat flow (×) during non-isothermal reaction of a stoichiometric PGE + aniline mixture at 1 °C min^{-1} (①) and 2.5 °C min^{-1} (②); simulation using the parameter set of Table 1 (—).

hydroxyl groups [17,23,26,29,30]. This method was used in Section 3.3.1 to a certain extent to obtain reasonable initial kinetic parameters. It is, however, restricted to model epoxy–amine systems in which the intermediate compounds can be synthesized. Another strategy consists of conceiving an explicit equation between the important rate constants and the concentrations of the functional groups. The equation can then be analyzed at certain conversions in the reaction path [9,12,13]. Finally, the differential equations can be solved by using a least sum of squares approach, which optimizes the experimental profiles in the entire conversion range [11,15,16,25]. As elaborated on before, the last strategy has been used here.

While the best simulation of both MTDSC signals and concentration profiles from HPLC is achieved by using the parameter set based on the mechanism in Section 3.1 (see also next section), a reaction mechanism without complexes, widely used in literature, is included for comparison (e.g.: case (i): see Fig. 8). Three parameter sets are shown in Table 2, each achieving an acceptable simulation for a restricted experimental input (techniques and signals, cure temperatures, mixture composition: indicated in Table 2). It turns out that, especially for mixtures having an excess in epoxide groups, an out of the ordinary substitution effect has to be presumed (compare case (i): 2.07 with case (ii): 0.58) to simulate the heat flow signal. Parameter sets (ii) and (iii) are in reasonable agreement with independent results from Mijovic et al. [15] and from Xu et al. [11,25].

The necessity to use the reaction mechanism in Scheme 1, including both reactive and non-reactive complexes, therefore becomes clear through using both the heat flow signal and heat capacity signal from MTDSC in the *complete* composition range.

3.4. Simulation of experimental results

The simulation capability of the optimized kinetic parameter set from Table 1 has to be checked to make sure that reaction exothermicity and concentration profiles are predicted over a wide range of cure temperatures and mixture compositions. It has to be stressed that all simulations are done with this parameter set to confirm the flexibility of the mechanistic approach in a wide range of experimental conditions (T_{cure} and composition). Optimizing the model for a specific experiment results in a closer fit but compromises the physical meaning of the kinetic parameters.

The effect of cure temperature is depicted in Figs. 10–13 for stoichiometric mixtures of PGE and aniline. Both the

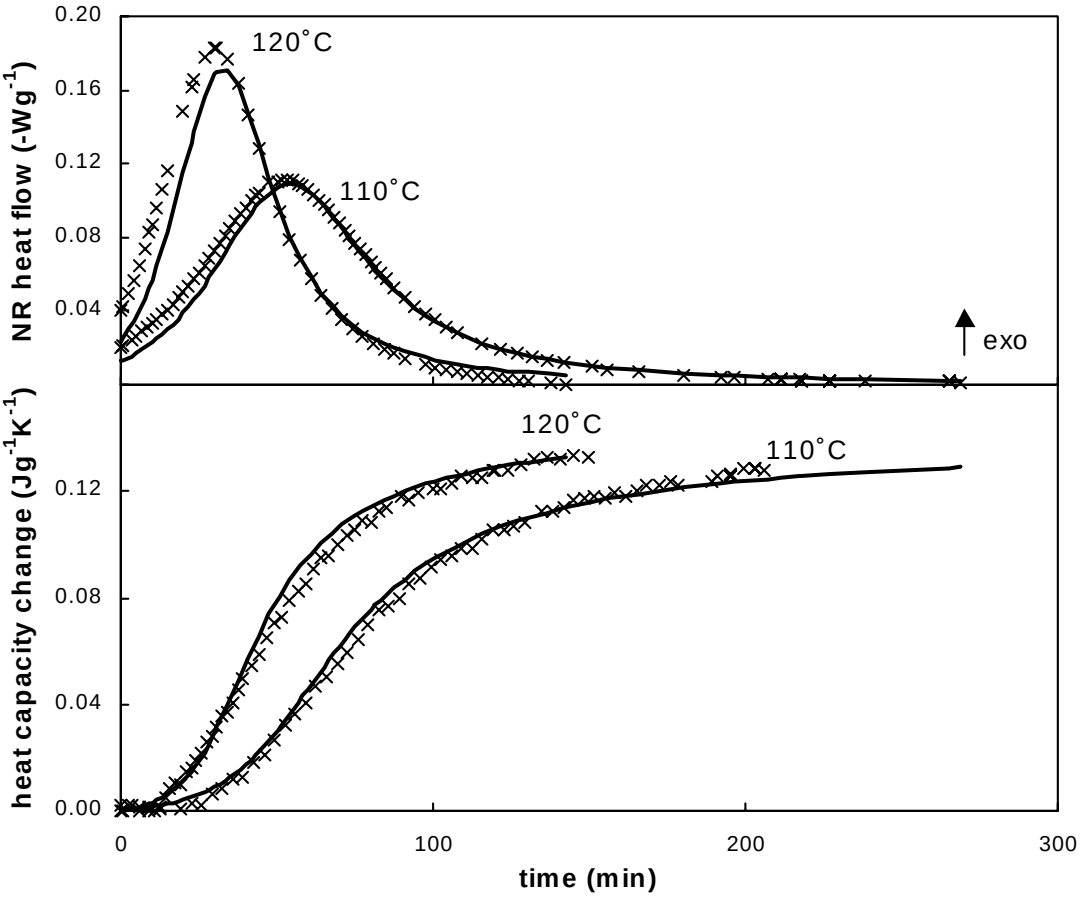

Fig. 12. Non-reversing (NR) heat flow (×) and heat capacity change (×) for the reaction of stoichiometric PGE + aniline mixtures at high reaction temperatures (110 and 120 °C); simulation using the parameter set of Table 1 (—).

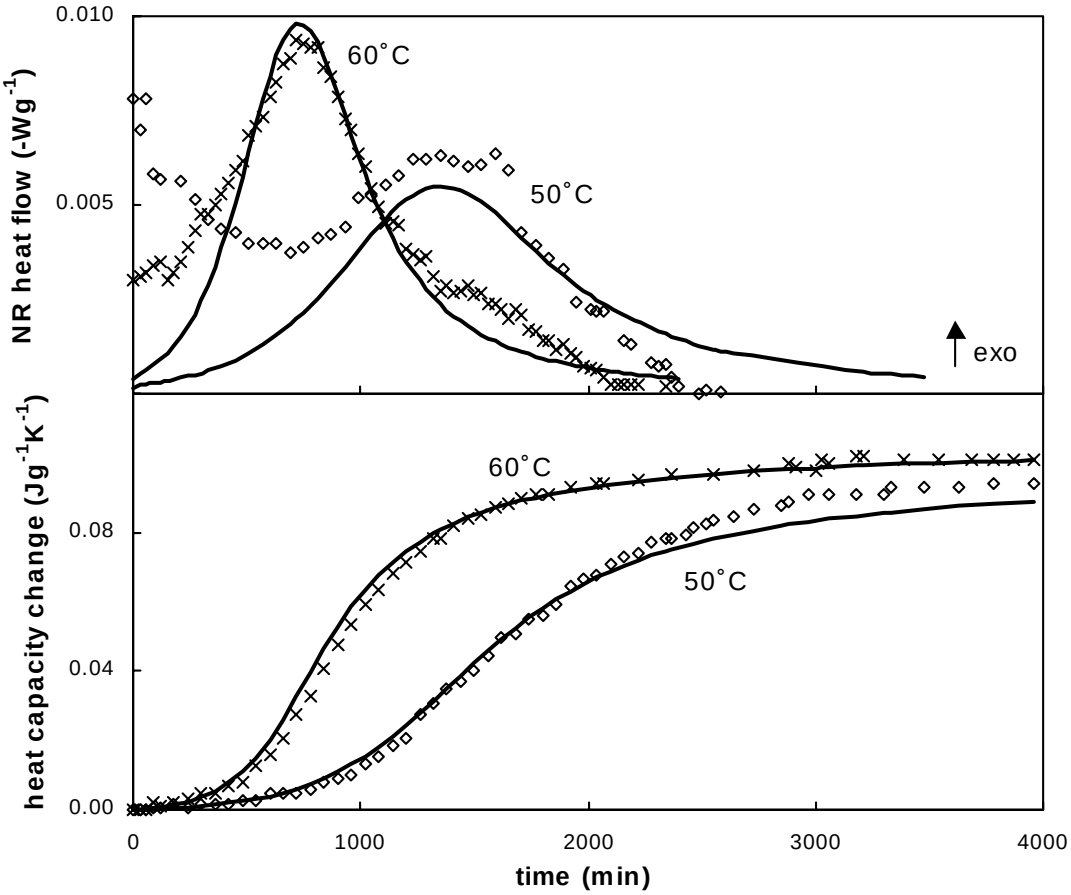

Fig. 13. Non-reversing heat flow and heat capacity change for the reaction of stoichiometric PGE + aniline mixtures at low reaction temperatures: 50 °C (◇) and 60 °C (×); simulation using the parameter set of Table 1 (—).

non-reversing heat flow and heat capacity change are depicted in Fig. 10 and show a good fit for reaction temperatures from 80 to 100 °C. Remind that the latter signal was estimated by using Eq. (6).

Both higher (non-isothermal cures in Fig. 11 and isothermal cures at 110 and 120 °C in Fig. 12) and lower T_{cure} (50 and 60 °C in Fig. 13) are simulated adequately. These show the flexibility and reliability of the proposed mechanism and kinetic parameters in predicting a temperature interval of 70 °C in T_{cure} with times to reach reaction completion ranging from 2 h at 120 °C until 3 days at 50 °C. At low cure temperatures, however, the long-term stability of the heat flow signal does not permit the reaction rate to be measured with sufficient accuracy. By performing a separate isothermal measurement of Sapphire at 60 °C, the peak-to-peak noise in the non-reversing heat flow was found to be 30 μW over 1000 min. This has to be compared to the small intensity of the non-reversing heat flow, as simulated in Fig. 13 to be at most 45 and 78 μW for 50 and 60 °C, respectively. Therefore, the non-reversing heat flow was not included as an experimental input for the optimization. The heat capacity signal, however, remains an accurate in situ tool to monitor the reaction of PGE + aniline as evidenced by the close correspondence with the predicted trend. Since this signal is calculated from the ratio between the amplitude of the cyclic component of the modulated heat flow and modulated temperature rate, it is more stable for long periods of time [53,54]. Moreover, not only the (low) reaction rate but also the evolution in concentrations of A_2 and A_3 determines the change in heat capacity (see Eq. (6)).

Simulated and experimental trends of the effect of mixture composition are illustrated in Fig. 14. Excess epoxy and amine in comparison to the stoichiometric PGE + aniline mixture at 100 °C result in a decrease and increase of the reaction rate, respectively (Fig. 14). The reaction heat capacity decreases with increasing amine concentration when calculated per mole of the minority component: 25 J mol^{-1} K^{-1} for both $r = 1$ and 0.7 and 22 J mol^{-1} K^{-1} for $r = 1.4$ at 100 °C (Fig. 14), resulting from the different $\Delta_r C_p$ contributions of primary and secondary amine–epoxy reaction steps [41].

The reaction of a stoichiometric PGE + A_2 mixture at 100 °C (Fig. 14, ④) can also be simulated with the parameters obtained from optimizing experimental data for the PGE + aniline system only. The reaction heat capacity from this secondary amine–epoxy reaction confirms the large difference in $\Delta_r C_p$ contribution: 36.5 J mol^{-1} K^{-1}. This was

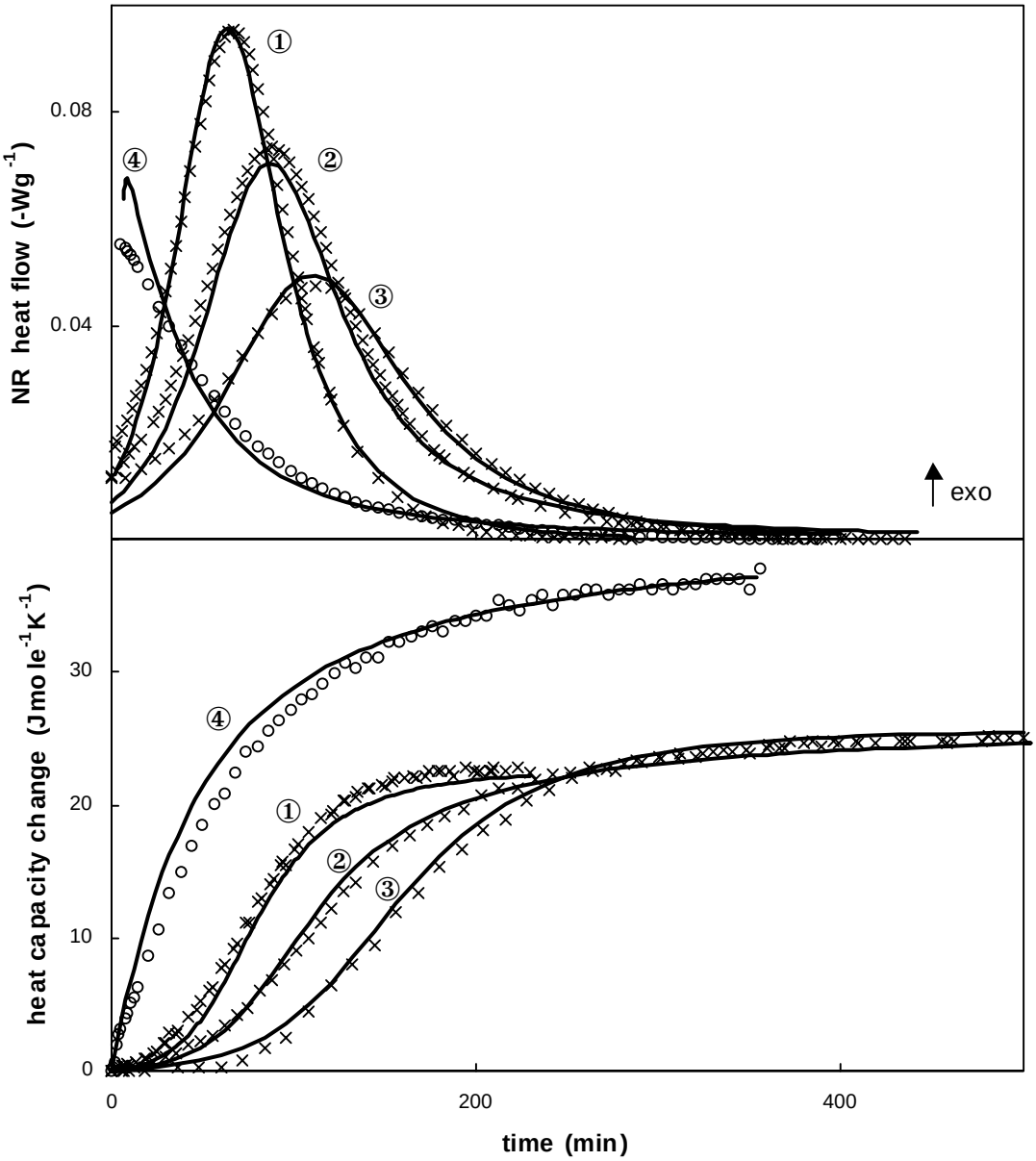

Fig. 14. Non-reversing (NR) heat flow and heat capacity change (normalized per mole of the minority component) for the reaction at 100 °C of PGE + aniline mixtures of different composition (×): $r = 1.4$ (①), $r = 1.0$ (②) and $r = 0.7$ (③) and for the reaction of a stoichiometric PGE + A_2 mixture (○) at 100 °C (④); simulation using the parameter set of Table 1 (—).

also evidenced in the non-linear behavior depicted earlier in Fig. 3.

The fact that the heat capacity signal is capable of providing information beyond the global conversion can be further confirmed by overlaying simulated and experimental concentration profiles (Fig. 15). While these experimental (HPLC/UV) profiles are not included as input signals in the optimization strategy, acceptable fits are found for all mixture compositions at 100 °C (consider experimental error of ±5–8%). When a higher initial concentration of A_1 is used, the primary amine–epoxy reaction is promoted, resulting in a higher maximum A_2 concentration.

The increase in reaction rate for amine concentrations more than twice as high as those in the stoichiometric case can still be simulated adequately as evidenced in Fig. 16 (②). A lower reaction temperature was chosen for the mixture with the highest amine excess to assure that the initial reaction rate would not be lost in the equilibration time.

The ability of DSC to measure the global reaction rate in situ while imposing a well defined cure schedule can therefore be extended to include information on the individual amine–epoxy reactions when using the heat capacity signal from MTDSC. While the concentration profiles for the individual components as obtained from HPLC or spectroscopic techniques can impose more restrictions on a mechanistic approach, the excellent temperature control and possibility to obtain *continuous* heat flow and heat capacity information with MTDSC are merits of this technique.

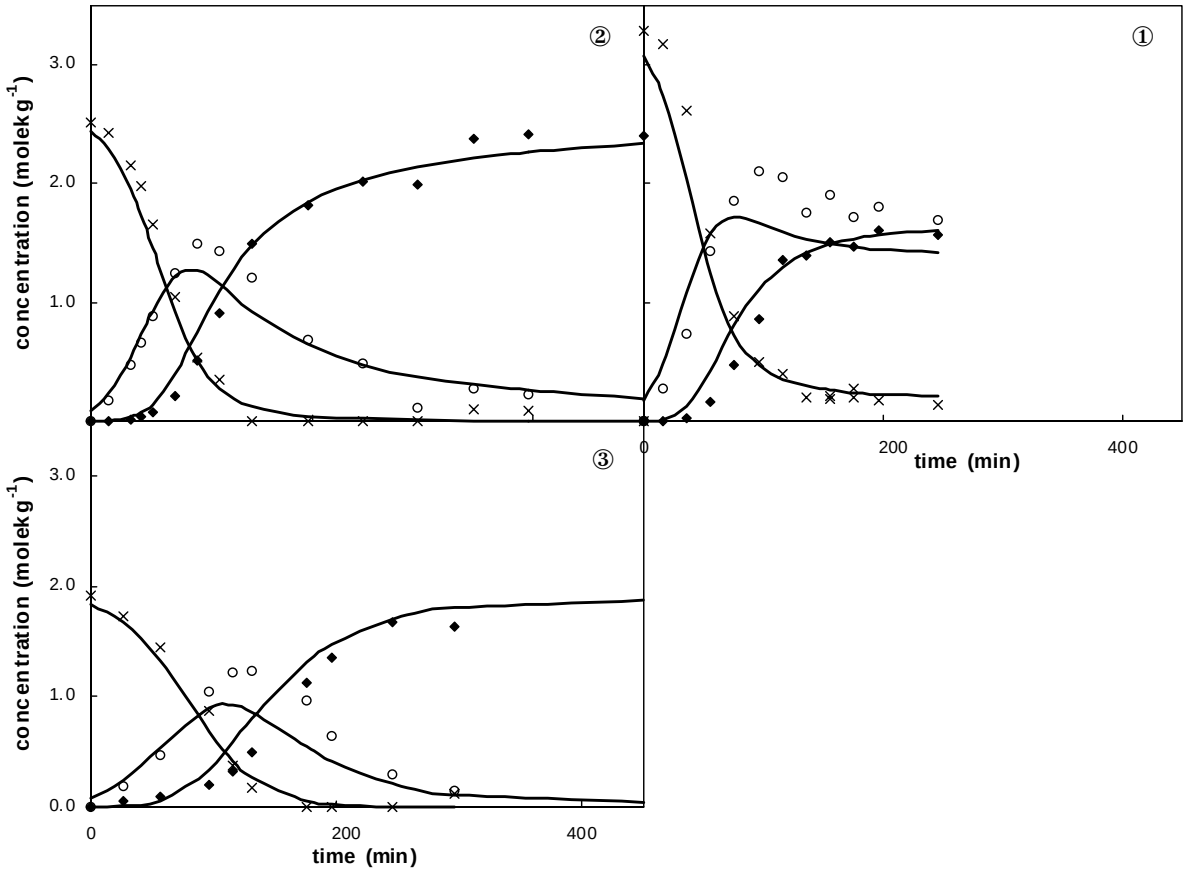

Fig. 15. Evolution of the concentration of aniline [A_1] (×), the secondary amine [A_2] (○) and the tertiary amine [A_3] (◆) as measured by HPLC at 100 °C for three mixture compositions: $r = 1.4$ (①), $r = 1.0$ (②) and $r = 0.7$ (③);simulation using the parameter set of Table 1 (—).

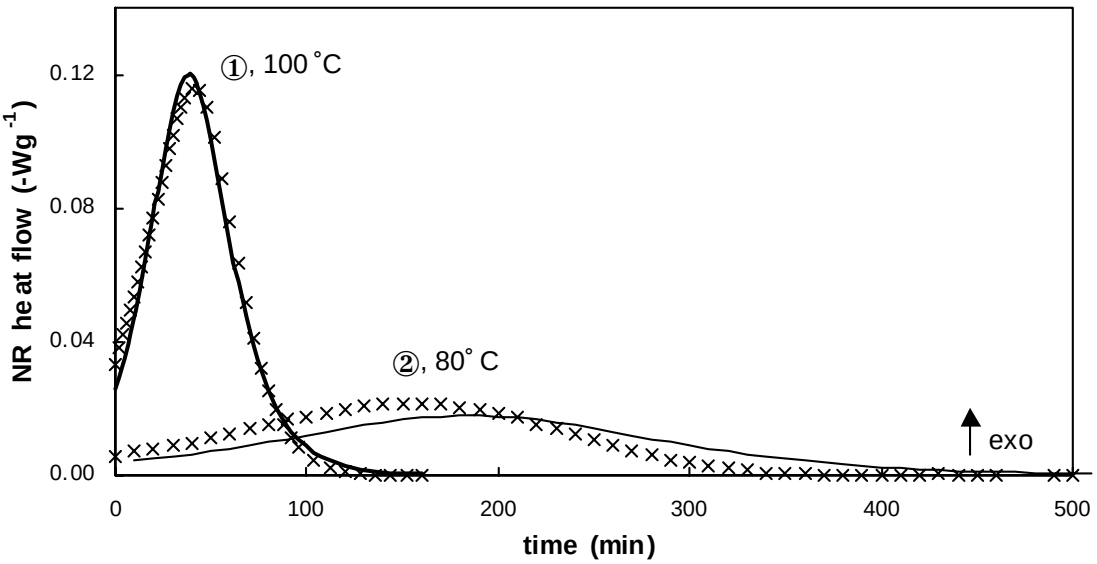

Fig. 16. Non-reversing heat flow (×) for the reaction of PGE + aniline mixtures with large amine excess: $r = 2.3$ at 100 °C (①) and $r = 5$ at 80 °C (②); simulation using the parameter set of Table 1 (—).

4. Conclusions

The constant relationship between the conversion calculated from the running integral of the heat flow signal and from separate chromatographic measurements confirms the commonly used assumption that both amine–epoxy reactions contribute equally to the reaction enthalpy. A non-linear behavior is found for the change in heat capacity, expressing the fact that at the useful reaction temperatures the reaction heat capacity of the primary-amine epoxy reaction is smaller than that of the secondary amine. Thus, while the global epoxy conversion can be extracted directly from the heat flow signal, the heat capacity signal can be used to disentangle both reaction steps. Moreover, reactions at low cure temperatures, for which the reaction rate is too small to be detected in the former signal, can still be obtained from the latter.

In this work, the change in heat capacity has been used for the first time as an input signal for mechanistic modeling of the PGE + aniline reaction. The consumption (production) rates and concentration profiles of the reactive species as obtained from the kinetic model are combined with the reaction enthalpies and heat capacities based on a group additivity approach to simulate the MTDSC signals. A temperature dependency had to be included for the reaction heat capacity in the range of cure temperatures since the additivity approach only predicts values at 25 °C. Using a least sum of squares optimization method, kinetic parameters are obtained that are able to simulate both MTDSC signals for different isothermal and non-isothermal experiments over a wide range of PGE + aniline mixture compositions. Moreover, direct concentration profiles obtained from chromatographic measurements can also be described adequately, confirming that not only the global reaction rate is well predicted, but also that of the individual amine–epoxy reaction steps (including the obtained negative substitution effect) is reliable.

The initial reaction rate has been found to depend in second order on the aniline concentration, confirming that the primary amine itself forms a complex with the epoxy prior to reaction. After these initial stages, the reaction rate is dominated by the primary and secondary amine reaction with (reactive) epoxy–hydroxyl complexes. Non-catalytic steps or side reactions like etherification and homopolymerization are not important in the PGE + aniline system. The reaction mechanism had to be complemented, however, with non-reactive complexes between hydroxyl and primary amine and the ether group of the epoxy. While the equilibrium constants of these steps were supposed to be independent of reaction temperature, this temperature dependence can be easily included in the present model when additional experimental data would become available. The flexibility of the mechanistic model will be further extended to include more commercially interesting epoxy resins [55].

Acknowledgements

The work of S. Swier was supported by grants of the Flemish Institute for the Promotion of Scientific-Technological Research in Industry (I.W.T.). The authors wish to thank Gabriella Török (Department ORGC, Free University of Brussels) for her guidance on chromatography.

References

[1] M.R. Kamal, Polym. Eng. Sci. 14 (1974) 231.
[2] S. Vyazovkin, N. Sbirrazzuoli, Macromolecules 29 (1996) 1867.
[3] G. Van Assche, A. Van Hemelrijck, H. Rahier, B. Van Mele, Thermochim. Acta 286 (1996) 209.
[4] G. Van Assche, S. Swier, B. Van Mele, Thermochim. Acta 388 (2002) 327.
[5] K. Horie, H. Hiura, M. Sawada, I. Mita, H. Kambe, J. Polym. Sci. Part A-1 8 (1970) 1357.
[6] K.C. Cole, Macromolecules 24 (1991) 3093.
[7] G. Wisanrakkit, J.K. Gillham, J. Appl. Polym. Sci. 41 (1990) 2885.
[8] N.A. St John, G.A. George, Progr. Polym. Sci. 19 (1994) 755.
[9] J. Charlesworth, J. Polym. Sci., Polym. Symp. Ed. 53 (1975) 45.
[10] X. Wang, J.K. Gillham, J. Appl. Polym. Sci. 43 (1991) 2267.
[11] L. Xu, J.H. Fu, J.R. Schlup, Ind. Eng. Chem. Res. 35 (1996) 963.
[12] P. JohnCock, L. Porecha, G.F. Tudgey, J. Polym. Sci.: Part A 23 (1985) 291.
[13] P. JohnCock, J. Polym. Sci.: Part A 27 (1989) 647.
[14] J.A. Marsella, W.E. Starner, J. Polym. Sci.: Part A 38 (2000) 921.
[15] J. Mijovic, A. Fishbain, J. Wijaya, Macromolecules 25 (1992) 979.
[16] H.J. Flammersheim, Thermochim. Acta 310 (1998) 153.
[17] N.S. Bedenyapina, V.P. Kuzenetsova, V.V. Ivanov, A.N. Zelenetskii, G.V. Rakova, L.A. Plokhotskaya, A.T. Ponomarenko, V.G. Shevchenko, N.S. Enikolopyan, Bull. Acad. Sci. USSR (Division of Chemical Science) 25 (1976) 1839.
[18] M. Fedtke, Makromol. Chem., Macromol. Symp. 7 (1987) 153.
[19] K. Fryauf, V. Strehmel, M. Fedtke, Polymer 34 (1993) 323.
[20] B.A. Rozenberg, Adv. Polym. Sci. 75 (1986) 113.
[21] L. Shechter, J. Wynstra, R.P. Kurkjy, Ind. Eng. Chem. 48 (1956) 94.
[22] I.R. Smith, Polymer 2 (1961) 95.
[23] Kh.A. Arutyunyan, A.O. Tonoyan, S.P. Davtyan, B.A. Rozenberg, B.A. Enikolopyan, Vysokomolekulyarnye Soedineniya A17 (1975) 1647.
[24] G.J. Buist, A.J. Hagger, B.J. Howlin, J.R. Jones, M.J. Parker, J.M. Barton, W.W. Wright, Polym. Commun. 31 (1990) 265.
[25] L. Xu, J.H. Fu, J.R. Schlup, J. Am. Chem. Soc. 116 (1994) 2821.
[26] N.S. Enikolopiyan, Pure Appl. Chem. 48 (1976) 317.
[27] G.J. Buist, J.M. Barton, B.J. Howlin, J.R. Jones, M.J. Parker, J. Mater. Chem. 6 (1996) 911.
[28] V. Spacek, J. Pouchly, J. Biros, Eur. Polym. J. 23 (1987) 377.
[29] Kh.A. Arutyunyan, E.A. Dzhavadyan, A.O. Tonoyan, S.P. Davtyan, B.A. Rozenberg, N.S. Enikolopyan, Russ. J. Phys. Chem. 50 (1976) 1212.
[30] B.A. Rozenberg, Fibre Sci. Technol. 19 (1983) 77.
[31] M. Younes, S. Wartewig, D. Lellinger, B. Strehmel, V. Strehmel, Polymer 35 (1994) 5269.
[32] E. Mertzel, J.L. Koenig, Adv. Polym. Sci. 75 (1986) 73.
[33] V. Strehmel, T. Scherzer, Eur. Polym. J. 30 (1994) 361.
[34] R.J. Varley, G.R. Heath, D.G. Hawthorne, J.H. Hodgkin, G.P. Simon, Polymer 36 (1995) 1347.
[35] J. Mijovic, S. Andjelic, Macromolecules 28 (1995) 2787.
[36] R.E. Lyon, K.E. Chike, S.M. Angel, J. Appl. Polym. Sci. 53 (1994) 1805.

[37] S. Swier, Reaction kinetics modeling and reaction-induced phase separation of epoxy–amine systems by means of modulated temperature DSC, Ph.D. Thesis, Vrije Universiteit Brussel, Belgium, 2002.
[38] J. Mijovic, S. Andjelic, Macromolecules 29 (1996) 239.
[39] J.M. Barton, Adv. Polym. Sci. 72 (1985) 111.
[40] G. Lachenal, N. Poisson, H. Sautereau, Macomol. Symp. 119 (1997) 129.
[41] S. Swier, B. Van Mele, J. Polym. Sci.: Part B 41 (2003) 594.
[42] U. Gaur, B. Wunderlich, J. Phys. Chem. Ref. Data 11 (1982) 313.
[43] G. Huybrechts, G. Van Assche, Comp. Chem. 22 (1998) 413.
[44] T. Turányi, Comp. Chem. 14 (1990) 253.
[45] B.A. Gottwald, G. Wanner, Simulation 37 (1982) 169.
[46] VA05, Harwell Subroutine Library, Release 11, AEA Technology, England, 1993.
[47] S.W. Benson, J.H. Buss, J. Chem. Phys. 29 (1958) 546.
[48] M. Luria, S.W. Benson, J. Chem. Eng. Data 22 (1977) 90.
[49] E.S. Domalski, E.D. Hearing, J. Phys. Chem. Ref. Data 22 (1993) 805.
[50] P. Barusch, J. Am. Chem. Soc. 75 (1953) 1987.
[51] C.C. Riccardi, F. Fraga, J. Dupuy, R.J.J. Williams, J. Appl. Polym. Sci. 82 (2001) 2319.
[52] Kh.A. Arutyunyan, A.O. Tonoyan, S.P. Davtyan, B.A. Rozenberg, N.S. Yenikolopyan, Vysokolmolekulyarnye Soedineniya A 17 (1975) 1647.
[53] B. Wunderlich, Y. Jin, A. Boller, Thermochim. Acta 238 (1994) 277.
[54] G. Van Assche, E. Verdonck, B. Van Mele, J. Thermal Anal. Calorimetry 59 (2000) 305.
[55] S. Swier, B. Van Mele, J. Appl. Polym. Sci., accepted for publication.